Synthesis of Li-ion battery cathode materials via freeze granulation

by

Keivan Amiri Kasvayee

Diploma work No. 72/2011

At Department of Materials and Manufacturing Technology

CHALMERS UNIVERSITY OF TECHNOLOGY

Gothenburg, Sweden

Diploma work in the Master program Advanced Engineering Materials

Performed at: Swerea IVF AB.
PO Box 104, 431 22, Mölndal, Sweden

Supervisors: Ola Lyckfeldt,
Swerea IVF AB, Material applications – Ceramics, PO Box 104, 431 22, Mölndal, Sweden
Jessica Orlenius
Swerea IVF AB, Material applications – Ceramics, PO Box 104, 431 22, Mölndal, Sweden

Examiner: Assistance Prof. Elis Carlström
Department of Materials and Manufacturing Technology
Chalmers University of Technology, SE-412 96 Gothenburg

Synthesis of Li-ion battery cathode materials via freeze granulation

Keivan Amiri Kasvayee

Diploma work no 72/2011
Department of Materials and Manufacturing Technology
Chalmers University of Technology
SE-412 96 Gothenburg
Sweden
Telephone + 46 (0)31-772 1000

[CHALMERS Reproservice]
Gothenburg, Sweden 2011

Synthesis of Li-ion battery cathode materials via freeze granulation
Keivan Amiri Kasvayee
Department of Materials and Manufacturing Technology
Chalmers University of Technology

Summary

Recently, enormous efforts have been done within the development of Li-ion batteries for use in portable electric devices from small scale applications such as mobile phones, digital cameras, laptop computers, to large scale applications like electrical vehicles (EVs) and hybrid electric vehicles (HEVs). $LiFePO_4$ as an active material in cathode materials in Li-ion batteries has shown outstanding advantages compare to other cathode materials such as low cost, low toxicity and environmental compatibility, good thermal stability, high theoretical specific capacity of 170 mAh/g and operating reversibility at 3.4V. Still, it is a need to develop the manufacture of the cathode material to achieve improved performance reliability by using environmental sustainable processes in order to meet future demands in large scale production and uses of Li-ion batteries.

The aim of this work was to develop a non-toxic, cheap, efficient and environmentally friendly process for synthesis of high quality active cathode material based on $LiFePO_4$ for Li-ion batteries. Water based suspensions/solutions containing various reactant constituents have been homogenized, granulated and calcined. Freeze granulation was applied as the key tool for the synthesis of $LiFePO_4$ with integrated carbon in order to produce granules with high degree of homogeneity prior to calcination. The resulting powder materials have been evaluated by XRD, carbon and conductivity measurements and characterization of other physical properties such as density and specific surface area. The promising version was used for manufacture of cathode material by tape casting, cell assembling and evaluation of the performance by charge/discharge cycling of the cells.

For the best sample in our experiment the XRD results revealed a high degree of purity, homogeneity and crystallinity of $LiFePO_4$. The produced $LiFePO_4$/C composite also had a high specific surface area and, therefore, considered as a promising material for cathode manufacturing and cell assembly. A discharge capacity of 155 and 140 mAh/g was achieved at the fifth cycle at 0.1C rate at room temperature for the cathodes which were made with NMP (solvent based) and water system, respectively. The long-term stability test indicated good result with no loss in capacity for at least 390 cycles. The satisfactory discharge capacity should be attributed to the homogenous nano-sized particles with a conductive porous carbon structure that was provided by the freeze granulation process and adapted calcination process.

Keywords: Li-ion batteries, $LiFePO_4$, cathode active material, specific capacity, freeze granulation, calcination, $LiFePO_4$/C composite, cell assembly.

Table of Contents

1. Introduction

Nowadays, there is a wide range of portable device applications from tiny scale applications like wireless autonomous devices, to large scale applications like electrical vehicles (EVs) and hybrid electric vehicles (HEVs) where efficient electrical power is of essential importance. Since all these equipments need to be powered by portable energy, the twenty-first century has sometimes been called "The Portable Age".

A battery is an electrical energy source that converts stored chemical energy into electrical energy. The lithium battery family is a group of batteries that contain lithium metal in their negative electrode. In present day common Li transition compounds such as $LiCoO_2$, $LiNiO_2$, $LiMn_2O_4$ and $LiFePO_4$ are used as cathode material in battery cell production, and they have shown a good performance during charge and discharge cycling.

Since 1997, when Padhi et al reported the first reversible lithium insertion-extraction for $LiFePO_4$ [1], it became one of the most interesting materials to be used as cathode material in lithium ion batteries. $LiFePO_4$ has outstanding advantages compare to other cathode materials like low-cost, low toxicity and environmental compatibility, good thermal stability, high theoretical specific capacity of 170 mAh/g and operating reversibility at 3.4V. This makes it as a strong potential candidate as positive electrode material in the next generation of Li-ion batteries. However, poor performance at low temperature and high current density, poor electronic conductivity and slow Li^+ ion diffusion are some drawbacks that have limited its applications. Furthermore, much of the processing of $LiFePO_4$ cathode material is based on toxic solvents/compounds which are not environmental friendly and probably will restrict large scale manufacture according to strengthened regulations. Therefore, it is a need to develop more sustainable processing concepts. Many efforts have been done during recent years to overcome the disadvantages by improving the synthesis methods, adapted particle size and morphology and increase the conductivity of $LiFePO_4$ [2]. However, there is still a considerable challenge to produce rechargeable Li-ion batteries with sufficient quality with an effective, cheap and environmentally friendly process for the active electrode material in all stages of the battery cell production.

The aim of this work was to develop a non-toxic, cheap, efficient and environmentally friendly process for synthesis of high quality active cathode material based on $LiFePO_4$ for Li-ion batteries. Water based suspensions/solutions containing various reactant constituents have been homogenized, granulated and calcined. Freeze granulation was applied as the key tool for the synthesis of $LiFePO_4$ with integrated carbon in order to produce granules with high degree of homogeneity prior to calcination. The resulting powder materials have been evaluated by XRD, carbon and conductivity measurements and characterization of other physical properties such as density and specific surface area. The promising version was used for manufacture of cathode material by tape casting, cell assembling and evaluation of the performance by charge/discharge cycling of the cells.

2. Theory

2.1 Lithium Batteries

A battery is an energy source which can convert chemical energy to electrical energy that can be extracted at a certain voltage [3]. This electricity comes from the electrochemical reduction-oxidation (redox) reactions within the active electrode materials. These reactions cause a continuous transfer between anode (negative electrode) and cathode (positive electrode) of ions via an electrolyte and of electrons via an external circuit. The reacting substances (active materials) are usually integrated with the electrodes. During discharge of the battery, the active material in anode gets oxidized and releases electrons to the external circuit whereas the active material in the cathode gets reduced by accepting the electrons.

Electrochemical batteries are classified as primary (non-rechargeable) and secondary batteries (rechargeable) depending of the capability of being electrically recharged. After discharging, a secondary battery is recharged by applying electric current in the opposite direction of discharging.

Lithium-ion batteries are very common in consumer electronics. They are one of the most popular rechargeable batteries for portable devices, military applications, electric vehicles, and aerospace applications. They have advantages like high energy density, low self discharge rate, no memory effect (hold less charge after several recharging), high cell voltage and specific energy.

The lithium battery family derives its name from employment of the lithium metal in its negative electrode. Lithium is the lightest metal and the Li/Li^+ electrode has the highest electro-negative potential. Therefore, it can produce high voltage and energy in couple with a counter electrode. Unlike the primary lithium batteries where lithium is used as anode in the form of pure metal or alloyed (which are disposable), secondary lithium-ion cells usually have an intercalation compound like graphite as anode material. In intercalation compounds guest molecules can intercalate (be inserted) between solid layers of the compound by expanding the van der Waals gap between the layers. Lithium can be reversibly intercalated in graphite. The energy for this process is usually provided by charge transfer between the guest and the host solid. In case of $LiFePO_4$, the intercalation of Li^+ ions results in the change of the oxidation state of Fe^{2+} to Fe^{3+}.

The technology of high-energy Li-ion secondary batteries was introduced commercially by Sony in 1991, operating with "host lattices" for both anode and cathode [2]. Figure 1 shows the schematic operations of a typical Li-ion battery. The anode is graphite coated on a copper foil which can intercalate Li^+ in its layers during charging. The cathode is a lithium insertion compound, e.g. $LiFePO_4$, coated on an aluminum foil. Lithium ions move from the anode (graphite) to the cathode ($LiFePO_4$) during discharge, and back when charging. The effectiveness of lithium insertion-extractions depends on many

factors like the movement of ions in electrolyte, transport (diffusion) of electrons and ions in the electrode materials, availability of sites for Li^+ ions in the electrodes and the density of electrons [2].

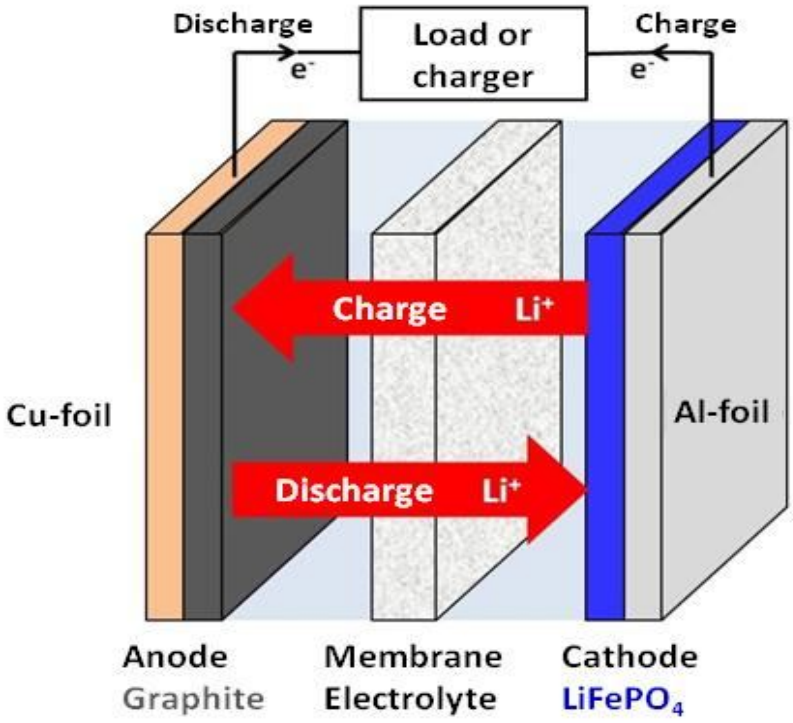

Cathode: $LiFePO_4 \leftrightarrow Li_{1-x}FePO_4 + xLi^+ + xe^-$

Anode: $xLi^+ + xe^- + 6C \leftrightarrow Li_xC_6$

Fig 1. Schematic illustration of a Li-ion electrochemical cell with lithium insertion compounds as both anode and cathode.

2.2 Present lithium based cathode materials

Common cathode materials of Li-ion batteries are the transition metal oxide based compounds such as $LiCoO_2$, $LiMn_2O_4$, $LiNiO_2$, $LiFePO_4$. Table 1 and Figure 2 show the basic properties of common Li compounds used for battery applications. $LiCoO_2$ has been the most common compound since 1991 when Sony, as the first company, commercialized it [2]. It is a 3.7V cathode material that shows good performance during long term cycling (>1000) with a practical specific capacity around 145 mAg^{-1}. However, it has some disadvantages like high cost, limited raw material availability, toxicity and large volume change during the redox reactions which will decrease the reversibility of the cell during cycling. $LiMn_2O_4$ and $LiNiO_2$ are also metal oxide based compounds that are used as an active material in Li-ion batteries displaying a specific capacity of 100 mA·h/g and 180 mA·h/g respectively. However, they show problems such as metastablity in fully charged cells and loss of oxygen at higher temperatures than 250°C, which may cause decomposition of the organic electrolyte and decrease the life time of

the cell. $LiMn_2O_4$ is cheaper, nontoxic and has better thermal capacity in comparison to $LiNiO_2$, but suffers from low practical specific capacity and rapid capacity fading, especially at high temperatures.

Table 1. Properties of common cathode materials in Li-ion batteries [2].

Electrode material	Nominal Voltage (V)	Theoretical specific capacity (mA·h/g)	Practical discharge capacity (mA·h/g)	Practical specific energy (W·h/kg)
LiCoO2	3.6	274	145	520
$LiMn_2O_4$	3.9	148	105	410
$LiFePO_4$	3.4	170	155	540
$LiNiO_2$	4.0	274	160	640

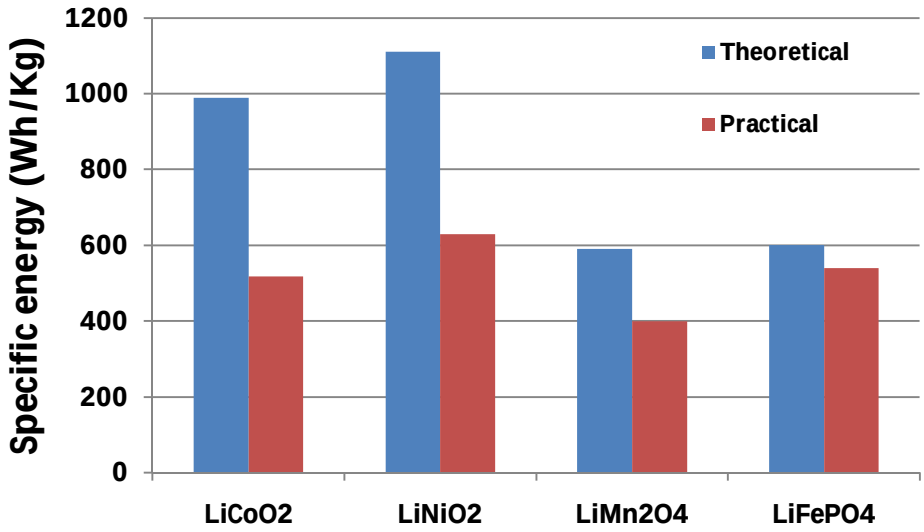

Fig 2. Comparison of specific energy (theoretical and practical) of common cathode materials in Li-ion batteries [2].

2.3 Lithium iron phosphate

Since 1997 when Padhi et al. reported that olivine structured lithium iron phosphate ($LiFePO_4$) can reversibly extract/insert Li ions, it became one of the most interesting cathode materials for Li-ion batteries [1]. Olivine $LiFePO_4$ has an orthorhombic crystalline phase with space group Pmnb. It has a hexagonal close packed arrangement and the crystal skeleton consist of FeO_6 octahedral and PO_4 tetrahedral [4]. In this structure the strong inductive effect of the PO_4^{-3} poly anion moderates a flat charge/discharge of 3.4 V between Fe^{+2}/Fe^{+3} and Li/Li^{+}. This arrangement provides a good mechanical and thermal stability with a theoretical density of 3.6 g/cm^3. Figure 3 schematically shows an olivine structured $LiFePO_4$.

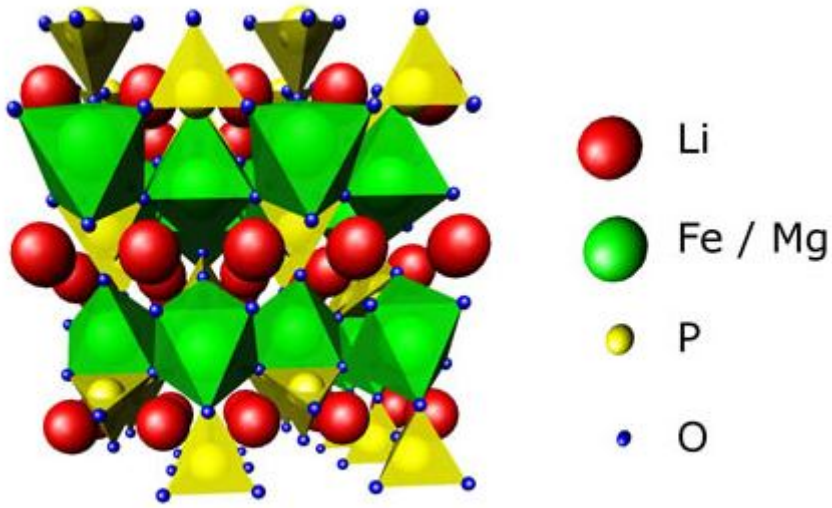

Fig 3. View of olivine structure of lithium iron/magnesium phosphate along an axis of the crystal structure [5].

$LiFePO_4$ exhibits useful characteristic for active cathode materials such as environmentally benign and none toxicity, low cost, thermal stability, excellent cycle properties with high reversibility of redox reaction, high specific capacity of 170 $mAhg^{-1}$ and an operating voltage of 3.4 V which made it to a promising cathode material for large scale applications. However, its performance is relatively poor at low temperatures and high current densities that prevent it from being used in all kind of applications. Lithium iron phosphate also suffers from its poor electronic and ionic conductivity as well as slow Li^+ ion diffusion in its structure during the redox reactions. These limitations have been improved relatively by using better methods of synthesizing including the use of conductive coating and ionic substitution to enhance its electrochemical properties [6].

2.4 Synthesis of LiFePO4

Several different methods have been investigated by researchers for synthesis of $LiFePO_4$. These methods provide various impacts upon several factors such as purity, crystal phase formation, particle size, particle size distribution and morphology that have a high influence on the electrochemical properties of the active material [2]. So the importance of the synthesis route and concept for producing the active material is of considerable importance.

At present time the main obstacle for reaching the theoretical capacity performance of $LiFePO_4$ is its very low electronic conductivity. Two approaches have recently been attempted to overcome the mentioned problem [7-10]. One approach is to enhance the electronic conductivity by adding conductive additives, e.g. adding carbon for the synthesis of a $LiFePO_4/C$ or selective coating with ionic doping. Another approach is to control the particle size, morphology and homogeneity by optimizing the synthesis

conditions. It has been reported that adding carbon as a polymeric material that can decompose into carbon under the annealing conditions is one of the most effective solutions. Carbon hinders grain growth during the formation of crystalline phase in the calcination process and enhances the ionic/electronic conductivity of the $LiFePO_4$ through improved contacts between particles. Additionally, the presence of carbon during calcination creates reducing conditions that limits the change of iron-valency ($Fe^{2+} \rightarrow Fe^{3+}$) that otherwise will degrade the material composition and performance [19, 20, 23].

Table 2 shows the precursors that are commonly used for $LiFePO_4/C$ synthesis. Lithium carbonate and hydroxide, ferrous salts such as acetate, oxalate and phosphate and $NH_4H_2PO_4$ or $(NH)_4H_2PO_4$ are the most common precursors that have been used for synthesis of $LiFePO_4$. Also, organic materials such as PVA (polyvinyl alcohol), PEG (polyethylene glycol) and citric acid that can decompose effectively into carbon during the annealing process have been explored as promising carbon precursor for the synthesis of $LiFePO_4/C$.

A variety of methods such as solid-state (ceramic), mechanical activation, aqueous co-precipitation, sol-gel, spray-pyrolysis and hydrothermal have been employed for synthesis of $LiFePO_4$. The chemical reaction between Li, Fe and P happens during solid state or liquid/solution/sol-gel conditions and results in the formation of amorphous $LiFePO_4$. The thermo-gravimetric (TGA) and differential thermal analysis (DTA) test show that the crystallization transition temperature of $LiFePO_4$ is between 450-570°C[2,11,14]. Thus, the initial amorphous sample will be calcined (also referred as annealing, sintering, thermal treatment) for enough time at temperatures higher than 450°C to get the crystalline $LiFePO_4$. The same approaches are used for synthesis of $LiFePO_4/C$ except addition of carbon precursors before the calcination step. A typical process using solid-state reaction for synthesis of $LiFePO_4/C$ reported by Mi et al. is as follow: Stoichiometric amount of $FePO_4.4H_2O$ and $LiOH.H_2O$ were wet ball milled and required amount of polypropylene (reductive agent and carbon source) were mixed into them and, after drying, calcined for 10h in N_2 atmosphere at several temperatures from 500 to 800°C to form $LiFePO_4/C$. They reported that TGA/DTA results shows formation of $LiFePO_4$ crystals and pyrolysis of polypropylene occurs in the same temperature range of 450-475 that shows the possibility of in-situ carbon coating during the synthesis [15].

Table 2. Li, Fe and P common precursors for synthesis of $LiFePO_4/C$.

Li precursor	Fe precursor	P precursor	Carbon precursor
LiOH	Fe_2O_3	$(NH_4)_3PO_4$	carbon black
LiOH.H2O	Fe_3O_4	$NH_4H_2PO_4$	PVA
Li_2CO_3	$Fe(C_2H_3O_2)_2$	$(NH_4)_2HPO_4$	sucrose
Li_3PO_4	$FeOH(C_2H_3O_2)_2$	$FePO_4.2H_2O$	glycol
$LiNO_3$	$FeSO_4$		polypropylene
	$FeC_2O_4*2H_2O$		
	$Fe(NO_3)_3$		
	$FePO_4$		
	$Fe_3(PO_4)_2$		
	$FePO_4.2H_2O$		

2.5 Preparation of cathodes and battery cells

The cathode electrode normally consists of the active material (e.g $LiFePO_4$), an additive like carbon black that further enhances the electronic conductivity and a binder like PVDF (polyvinylidene fluoride) in order to promote the adhesion of the cathode material to the substrate metal foil. A suspension/paste with all the ingredients is prepared and applied upon the metal foil as a thin layer using tape casting or similar techniques. Since the binder and conductive agent are usually electrochemically inactive materials, their presence will decrease the total specific energy of the electrode and hence the cell. Therefore, it is desirable to minimize their amounts.

In traditional cathode production a large amount of organic solvent are used as medium for this process in order to make a homogenous mixture of the constituents and enable proper tape casting. The solvent predominantly used in the Li-Ion industry is N–methylpyrrolidone (NMP). Using NMP is undesirable because it has some disadvantages such as high cost, besides being volatile, flammable, easily absorbed by the human skin and suspected to cause genetic and reproductive damages to humans [16,17]. High manufacturing cost and environmentally concerns of using NMP and satisfactory stability of $LiFePO_4$ in water are hence the main reasons that make it necessary to develop aqueous routes in all stages of the manufacture of $LiFePO_4$ cathodes.

The properties of the anode material and the electrolyte are important and have a high influence on the performance of $LiFePO_4$-based lithium batteries. For example, the operating temperature has a remarkable influence on the viscosity of the electrolyte, rate of lithium ion diffusion as well as redox reaction kinetics which affect the cell performance to a great extent [2]. In most of the studies reported in literature $LiPF_6$ and lithium metal in cell production as electrolyte and anode, respectively have been used.

Such studies reveal high active material utilization, reasonably high rate-capability and good cycle properties for Li/ $LiFePO_4$-C cells at room temperature. Cell assembling is normally conducted under inert atmosphere with a low level of oxygen and water vapor. Any water must be removed from the electrode material before the cell production. Since the performance voltage of lithium-ion cells is much higher than the electrolysis voltage of water, water has a significant influence on the performance of the batteries [18].

2.6 Freeze granulation

As an essential tool in this work, freeze granulation was used within the synthesis of $LiFePO_4$ as well as in the subsequent cathode material preparation.

Swedish Ceramic Institute (SCI) developed Spray Freeze Drying (SFD) and Spray Freezing into Liquid (SFL) for granulation of ceramic powders in the 1980s and since then this process was called Freeze Granulation (FG). It has been observed that FG provides granules with better homogeneity and superior sintering performance of ceramics after pressing than other granulation methods do [19].

The freeze granulation process is based on instant freezing of sprayed droplet (granules) of a powder suspension into stirred liquid nitrogen and a subsequent freeze drying to remove the frozen liquid by sublimation. In this process granules size and density can be controlled by changing the powder concentration and adapt the atomizing airflow and suspension feed into the spray nozzle. Figure 4 schematically shows the freeze granulation process.

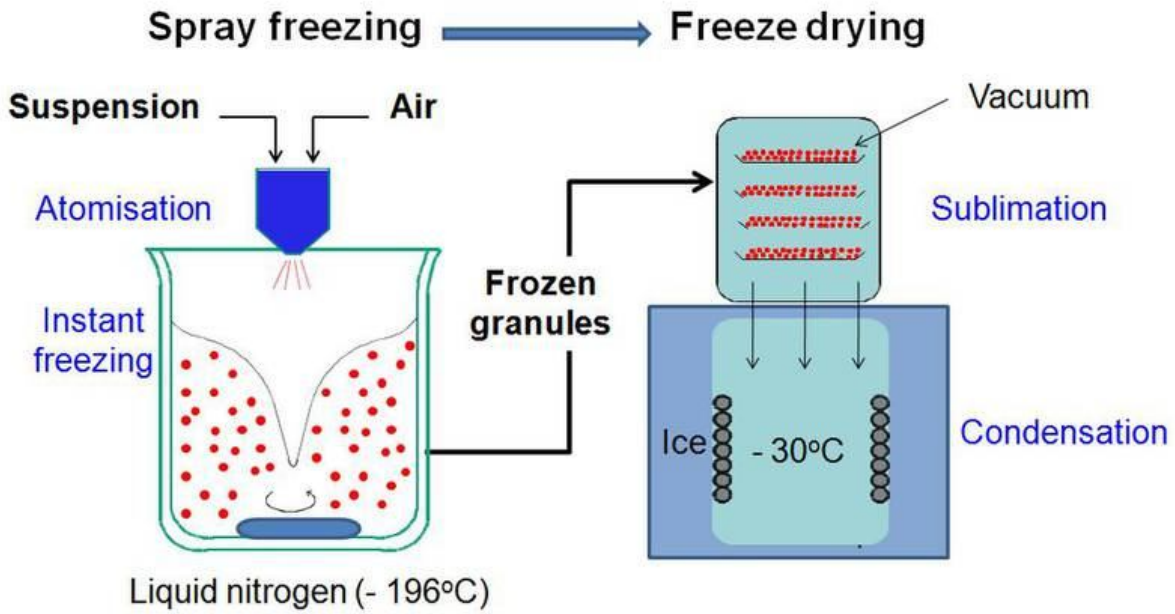

Fig 4. Schematic of the freeze granulation/freeze drying process [20].

During freeze drying, the solvent evaporates directly from frozen state (sublimation) without changing to liquid formation. As a result, many of the problems appearing when using other types of granulation methods (for example spray-drying), such as granule shrinkage and cavities, agglomeration, strong interparticle bonds, and migration of additives and/or smaller particles to the granule's surface, are avoided (see Figure 5). The FG process gives a high degree of granule homogeneity and a granule density corresponding to the powder concentration in the original suspension.

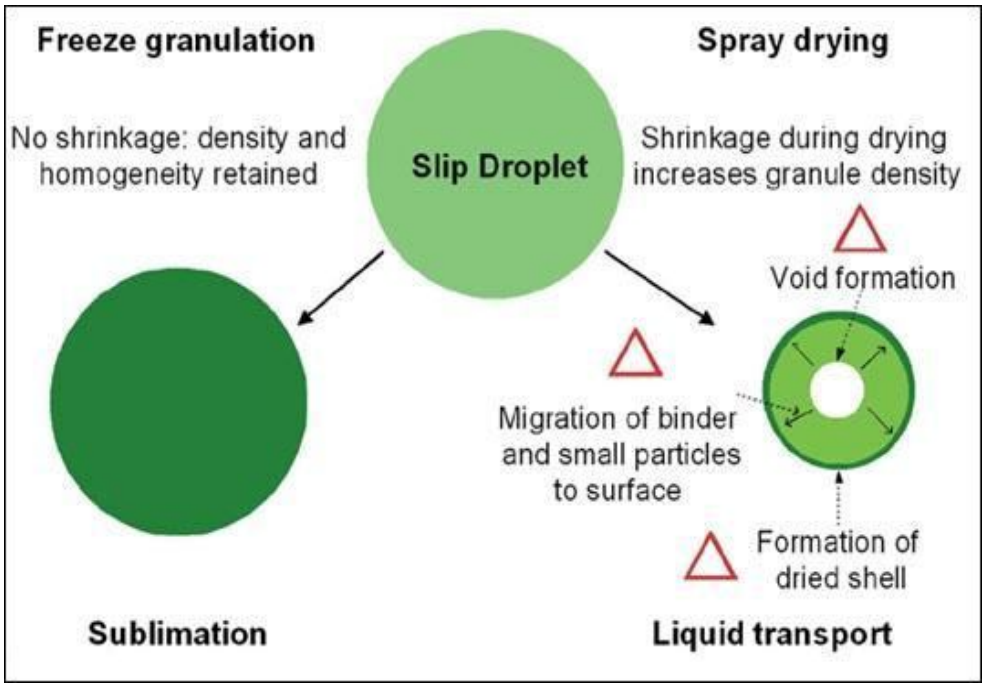

Figure 5. Comparison of the drying process in freeze granulation and spray drying [21].

The shape and size of the granules are related to the rheology of suspension (viscosity profile), flow rate of the suspension and pressure of the applied atomizing air. Suspensions with lower viscosity will produce smaller granules, however it can be altered by changing the suspension feed and air pressure [19]. Normally, granule size distribution in this process is between 50-400 μm. Freeze granulation can be used with water as well as a wide range of organic solvents that have a freezing point in the range of -25°C to +10°C. Solvent with lower freezing point inhibits the freeze drying process whereas those with freezing point higher than +10°C can cause clogging of the spray nozzle.

In this study the purpose to use FG was to preserve the homogeneity of wet milled mixes of precursors until calcination take place, considered essential for a maximized output of fine grained $LiFePO_4$ with accurate phase composition. Additionally, since no shrinkage of the granules or strong bonds within the granules is achieved with FG, a loose structure of fine particles is achieved. This is foreseen to support break down of granules into separated particles at milling as conducted at the suspension preparation for casting of the cathode material. Thus, freeze granulation was chosen as an ideal process and a key tool for this work.

3. Experimental

3.1 Raw materials

There is a wide spectrum of possible materials for solid-phase synthesis of $LiFePO_4$. However, it becomes a bit more limited if we consider their characteristics. For example, water solubility and a resulting high salt concentration affect the freezing behavior, which is especially important for the freeze-drying step in freeze granulation. Additionally, economical and environmental considerations led to the choice of the compounds listed in table 3 as the main starting material candidates.

Three different combinations of precursors were employed for production of $LiFePO_4$.In all three approaches, lithium carbonate (Li_2CO_3) was used as Li precursor. In the first mixture iron(II) oxalate dihydrate ($FeC_2O_4*2H_2O$) was used as iron precursor and Ammonium phosphate dibasic ($(NH_4)_2HPO_4$) as phosphate precursor. Iron(II) oxalate dihydrate ($FeC_2O_4*2H_2O$) and ammonium phosphate monobasic ($NH_4H_2PO_4$) were employed in the second combination as iron and phosphate source respectively. In the last and third combination, iron(III) phosphate dihydrate ($FePO_4.2H_2O$) was used as combined iron and phosphate precursor. All the powders were delivered by Sigma-Aldrich. Table 4 shows the precursors characteristics.

Table 3. Raw materials used in this study.

Product name	Formula	Brand	Product number
Lithium carbonate	Li_2CO_3	Sigma-Aldrich	13010
Iron(II) oxlate dihydrate	$FeC_2O_4.2H_2O$	Aldrich	307726
Ammonium phosphate dibasic	$(NH_4)_2HPO_4$	Fluka	9840
Ammonium phosphate monobasic	$NH_4H_2PO_4$	Sigma-Aldrich	A1645
Iron(III) phosphate dihydrate	$FePO_4.2H_2O$	Aldrich	436011

Polyvinyl alcohol (PVA, Mowiol 4-88, Clariant) was used as carbon source in order to producing $LiFePO_4/C$. Pyrolysis of PVA was expected to deposit a thin layer of carbon on simultaneously created $LiFePO_4$ particles in temperatures higher than 400°C. PVA solution was added prior to freeze granulation and calcination to restrict grain growth and create a reducing atmosphere that prevents the conversion from Fe^{2+} to Fe^{3+}, which favors conductivity.

Two commercial $LiFePO_4/C$ powders, named A and B in this study, were used for several evaluations as comparison for produced powders.

Table 4. Properties of precursors that have been used in this study.

Compound formula	Mol weight (g/mol)	Density (g/cm³)	Water solubility at 20°C	pH
Li_2CO_3	73.89	2.11	10 g/l	11
$FeC_2O_4*2H_2O$	179.89	2.28	Not	3.5
$(NH_4)_2HPO_4$	132.06	1.62	132.1 g/cm³	8.4
$NH_4H_2PO_4$	115.03	1.8	soluble	8
$FePO_4.2H_2O$	186.85	2.63	Not	4

3.2 Suspension preparation

$LiFePO_4$ suspensions were prepared via ball milling with stoichiometric molar ratio of the precursors according to the reaction equations given below. After completed milling and addition of all the reagents, an appropriate amount of PVA was added to the suspension during stirring prior to granulation.

Reaction equations

1) $Li_2CO_3 + 2\ FeC_2O_4*2H_2O + 2\ (NH_4)_2HPO_4 \Rightarrow 2\ LiFePO_4 +$ Gas products*
2) $Li_2CO_3 + 2\ FeC_2O_4*2H_2O + 2\ NH_4H_2PO_4 \Rightarrow 2\ LiFePO_4 +$ Gas products*
3) $Li_2CO_3 + 2\ FePO_4.2H_2O \Rightarrow 2\ LiFePO_4 +$ Gas products*

*Reasonably such as H_2O, CO and CO_2

I) In the first combination, aqueous suspensions of Li_2CO_3 and $FeC_2O_4*2H_2O$ were ball milled overnight, separately. In these suspensions 60% of total suspension volume was water. Table 5 presents the synthesis recipe for the first precursor combination. Since the $FeC_2O_4*2H_2O$ suspension had a lower pH (3.5) than the Li_2CO_3 suspension (pH=11), agglomeration may occur at mixing of the two. Therefore a small amount of ammonium (3g) was added to the $FeC_2O_4*2H_2O$ suspension to increase pH to 8.5. Then proper amounts of the two suspensions (see the wt% ratio at table 5) were mixed together and were ball milled overnight. After completed milling, the mixture suspension was separated from the balls and an appropriate amount of $(NH_4)_2HPO_4$ aqueous solution (15 wt% solid) was added to it during stirring. After 4 hours stirring the suspension was divided into two parts for further processing with or without PVA addition. 5 wt% of PVA based on solids was added in aqueous solution form to one part of the suspension and then stirred for another hour prior to granulation. Table 5 shows data of the precursors and synthesis recipe of the first combination.

Table 5. Synthesis recipe for the first precursor combination.

Precursor	**Li_2CO_3**	**$FeC_2O_4*2H_2O$**	**$(NH_4)_2HPO_4$**		
Mol weight (g/mol)	73.89	179.9	132.06		
Density (g/cm^3)	2.11	2.28	1.62		
Mol% in final suspension	20	40	40		
Wt% in final suspension	10.59	51.56	37.85		
Vol% in final suspension	9.84	44.34	45.81		
Suspension compositions	**Li_2CO_3**	**$FeC_2O_4*2H_2O$**	**$(NH_4)_2HPO_4$**	**PVA**	**total**
Precursor weight (g)	42.2	205.5	150.8	19.925	398.5
Precursor volume(ml)	20	90.1	93.1	16.7	219.9
Added water (ml)	30.2	135.2	865.8	99.6	1130.8
Suspension volume (ml)	50.2	225.3	958.9	116.3	1350.7

II) For the second combination an appropriate amount of Li_2CO_3 (30% volume solids), 1.52g (0.3wt% based on Li2CO3) Dolapix PC21 (Zschimmer & Schwarz) as dispersant and water were ball milled overnight. Table 6 shows the synthesis recipe for the second precursor combination. Then according to synthesis recipe proper amounts of water and $FeC_2O_4*2H_2O$ (40% volume solids) were added to Li_2CO_3 container and ball milled for one more night. After completed milling the mixture was separated from the balls and appropriate amount of $NH_4H_2PO_4$ aqueous solution (15% vol.) was added during stirring. The resulting suspension was stirred for 4 hour and then separated into four parts. PVA was added in aqueous solution form in 5, 6 and 7 weight percent based on solid content into three of the separated suspension batches and one batch was left without PVA. After one hour stirring, the suspension with and without PVA were freeze granulated.

Table 6. Synthesis recipe for the second precursor combination.

Precursor	**Li_2CO_3**	**$FeC_2O_4*2H_2O$**	**$NH_4H_2PO_4$**	
Mol weight (g/mol)	73.89	179.9	115.03	
Density (g/cm^3)	2.11	2.28	1.8	
Mol% in final suspension	20	40	40	
Wt% in final suspension	11.13	54.21	49.22	
Vol% in final suspension	10.92	34.66	39.86	
Suspension compositions	**Li_2CO_3**	**$FeC_2O_4*2H_2O$**	**$NH_4H_2PO_4$**	**total**
Precursor weight (g)	126.6	616.6	394.2	1137.4
Precursor volume(ml)	60	270.4	219	549.4
Added water (ml)	140	405.7	1241	1786.7
Suspnesion volume (ml)	200	476.1	1460	2136.1

III) The third suspension preparation procedure was quite similar to the second one. Table 7 shows the recipe for synthesis of the third precursor combination. After one night milling of Li_2CO_3 (30% volume solids) with dispersant and water, appropriate amounts of $FePO_4.2H_2O$ and water (see the wt% ratio at table 7) were added to the suspension and ball milled for one more night. PVA in amounts of 5, 6 and 7 wt% based on solids was added in separate batches. After one hour stirring the suspensions were ready for freeze granulation.

Table 7. Synthesis recipe for the third precursor combination.

Precursor	**Li_2CO_3**	**$FePO_4.2H_2O$**	
Mol weight (g/mol)	73.89	186.83	
Density (g/cm³)	2.11	2.63	
Mol% In final suspension	33.4	66.6	
Wt% in final suspension	16.55	83.45	
Vol% in final suspension	19.82	80.18	
Suspension compositions	**Li_2CO_3**	**$FePO_4.2H_2O$**	**Total**
Precursor weight (g)	158.66	800	958.66
Precursor volume(ml)	75.2	304.2	379.4
Added water (ml)	0	1723.7	1723.7
Suspension volume (ml)	75.2	2027.9	2103.1

3.3 Freeze granulation

The resulting stable suspensions of PVA and precursors were sieved (250 μm) and granulated via the freeze granulation process. The suspensions were atomized at an air pressure of 30 kPa and a suspension feed of 1 liter per hour utilizing a lab scale freeze granulator (LS-2, PowderPro AB). Figure 6 shows an image of the same type of granulator used in this study. Produced frozen granules were transferred to and dried in a freeze dryer (Lyovac GT2) via sublimation under vacuum condition. In a separate experiment the eutectic point of the media (the freezing point of the suspension) was investigated. The eutectic temperature can be measured by continuously cooling the media and simultaneously measuring both temperature and resistance [22]. The instant increase in suspension resistance shows the eutectic or freezing point. The freezing point of the first suspension was -16°C. Therefore, the vacuum pressure in the drier was set to 5.7 Pa, which corresponds to a temperature of -26°C that insured full sublimation of water from the frozen granules without any risk for melting. In addition, the dryer condenser temperature was -50°C to freeze and collect the evaporated water and prevent it from going to the vacuum pump. Dried granules were sieved (<355 μm) and stored for the calcination experiments.

Fig 6. Lab scale freeze granulator (LS-2, PowderPro AB, Sweden). [29]

3.4 Calcination

Calcination temperature is one of the most important parameter at synthesis of $LiFePO_4$ and has a large influence on the electrochemical properties. Calcination temperature can affect crystalline structure, particle size, particle distribution as well as the amount and structure of carbon coating attained. It has been reported that the crystallization temperature of amorphous $LiFePO_4$ is between 450-570°C [2,11]. Moreover, according to the reports PVA fully converts into aromatics and substituted olefins at pyrolysis temperatures higher than 400°C [23].

Therefore, the selection of an optimum calcination temperature should be in temperatures higher than 450°C. In many reports the active material that shows the highest performance was calcained between 600-800°C [11-13,24-27]. In addition, using inert or reducing atmosphere during calcination is necessary in order to prevent formation of undesirable Fe^{+3} compounds and avoid oxidation of the carbon residues [12]. Thus, in this study it was decided to choose the calcination temperatures in the mentioned range and use nitrogen or argon+10% hydrogen as atmosphere.

The furnace initially used for this purpose was equipped with a balance that enabled monitoring weight changes during calcination. The result from this was used to define the appropriate temperatures for the further calcination.

The first precursor combination containing 5% PVA was calcined in temperatures of 600, 700 or 800°C in nitrogen atmosphere using a heating rate of $1°Cmin^{-1}$ and a dwell

time of 10 hour. In addition, a small amount of precursor without PVA was calcined at the same temperatures for comparison.

Second and third precursor combination containing 5,6 and 7% PVA were calcined in nitrogen atmosphere at 650, 700 and 750°C with the same temperature schedule as previously used. To increase the reducing power of the furnace atmosphere, 700°C calcination was repeated in argon+10%hydrogen. This calcination was conducted in a graphite resistance furnace (Pfeiffer Balzer, vacuum sintering furnace, COV 373). This furnace was also used for the calcination of larger batches of powder based on the results of the three sets of concept evaluated. Table 8 summarizes the calcination conditions used for the three different precursors combination.

Table 8. Precursor's calcination temperature and atmosphere. Precursors groups consist of: (I) Li_2CO_3, $FeC_2O_4*2H_2O$ and $(NH_4)_2HPO_4$. (II) Li_2CO_3, $FeC_2O_4*2H_2O$ and $NH_4H_2PO_4$. (III) Li_2CO_3 and $FePO_4.2H_2O$. In all cases a 10 hours dwell was used.

Precursor	PVA (wt%)	Temperature (°C)	Atmosphere
I	5	600, 700, 800	N_2
II	5, 6 , 7	650, 700, 750	N_2 or Ar+10% H_2
III	5, 6, 7	650, 700, 750	N_2 or Ar+10% H_2

3.5 Evaluations

In this study surface area measurements according to the multi-point BET method (Gemini 2360, Micromeritics, US) were conducted and powder density was measured with a helium pycnometer (AccuPyc 1330, Micromeritics, US). An automatic elemental analyzer (made by Heraeus) was used in order to determine the amount of carbon coated on the $LiFePO_4$ particles. The device uses heating and a flow of pure oxygen to oxidize the carbon coating. The calculated amount of carbon dioxide that passed through the filters of the device expressed the amount of residual carbon in $LiFePO_4/C$ granules.

The crystal structures of the prepared samples were examined by powder X-ray diffraction (XRD) using a Bruker D8 Advance diffractometer with chromium tube. Scanned data were collected over the 2θ range of 20-130° and the step size was 0.1° with a counting time of 10 seconds. The microstructure of the $LiFePO_4$ and $LiFePO_4/C$ were investigated by field-emission scanning electron microscopy (Jeol, JSM-840A, SEM/EDX). The photos were taken with the magnification of 5000 by using secondary electron emission. In addition, elemental map analysis was applied in order to investigate the homogeneity and distribution of the comprising elements of $LiFePO_4/C$.

Conductivity of produced $LiFePO_4/C$ powder was examined by using pressed tablets of the calcined powder materials. For each tablet, 0.5 g powder was hydraulic pressed at

88MPa in a 12.56 mm diameter cylindrical tool and subsequently cold isostatic pressed (C.I.P. 42260, Avure technologies) at 300 MPa. Then the top and bottom surfaces of the tablets were coated with a silver paste (produce by NBE Tech, LLC) in order to gain a high conductivity of the surfaces and enable accurate conductivity measurement. Silver coated tablets were heated in nitrogen atmosphere at 150°C for 10 minutes to evaporate the solvent in the silver paste and then further up to 250°C to yield a pure silver layer on the tablet surfaces. The resistances of the silver coated tablets were investigated through their thickness by using a voltmeter. Figure 7 shows the setup of the conductivity measurement of a silver coated tablet. The conductivity was calculated by using the formula $\partial = {}^{L}/_{R \times A}$ in which ∂ is conductivity ($s.m^{-1}$), L is thickness (m), R is resistance (Ω) and A is cross-sectional area (m^2).

All described analyses were also conducted with the commercial $LiFePO_4$/C materials (A and B).

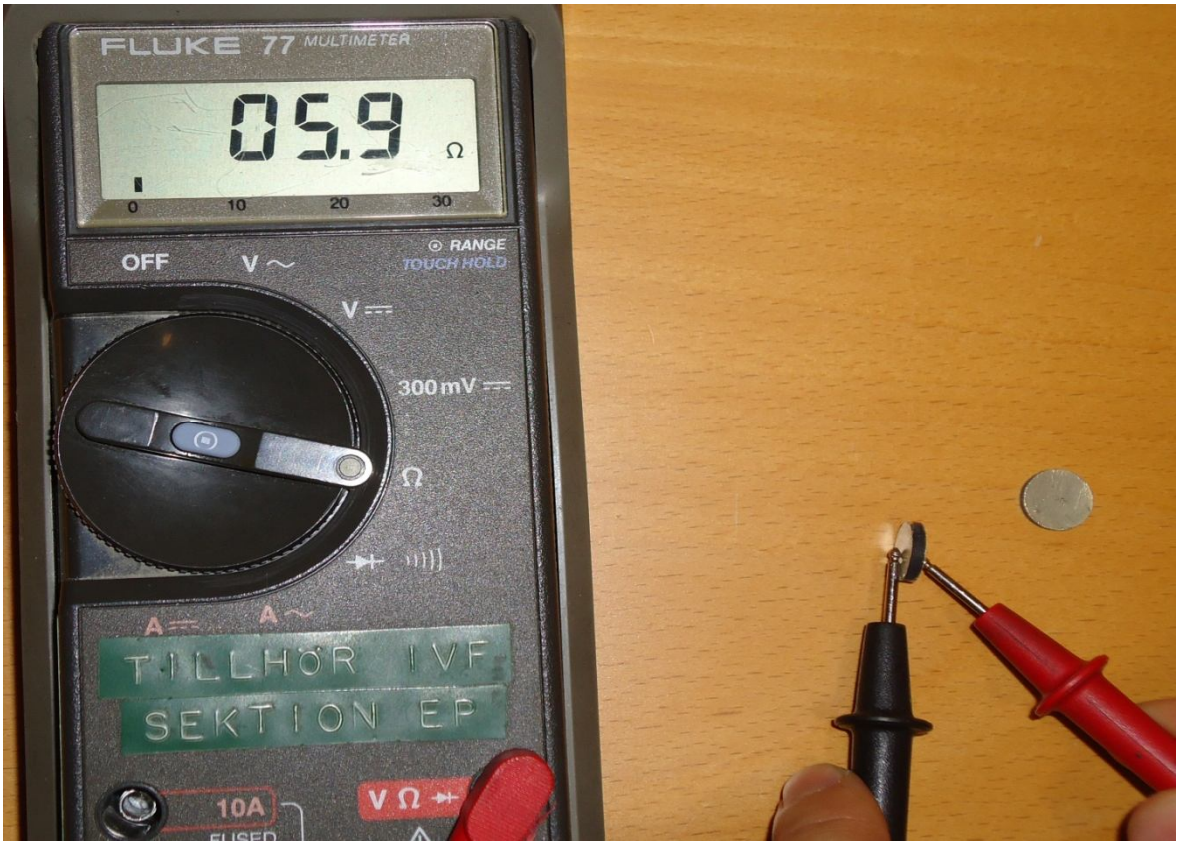

Fig 7. Experimental setup of conductivity measurement of a silver coated pressed tablet of $LiFePO_4$ powder.

3.6 Milling and granulation of calcined material

Based on the previous characterization, one chosen version of calcined $LiFePO_4/C$ material was ball milled in water over night and then freeze granulated prior to the cathode preparation step. This treatment was done in order to first break down the granules consisting of small primary particles, eventually strongly bonded together during calcination, and in the next step create soft granules by another FG step. Consequently, post milling and a subsequent FG was intended to give granules with improved wetability and promote the following cathode suspension preparation. Hence less solvent would be needed for suspension preparation and better coating of active material would be achieved. On the other hand, it may require more binder in order to obtain sufficient binding of the cathode materials and adhesion to the substrate foil considering higher exposed surface area.

3.7 Cathode preparation

Cathode materials were fabricated by manual tape casting with two different $LiFePO_4/C$ suspensions, based on water and N-methylpyrrolidone (NMP) respectively, on an aluminum foil (thickness: 16mm, LinYi Gelon New Battery Materials Co). The mixture with NMP contained 80 wt% $LiFePO_4/C$, 10 wt% carbon black (Super P-Li, Timcal) as conductive agent and 10 wt% PVDF binder (Kynar HSV 900, Arkema). The suspension based on water contained 85wt% $LiFePO_4/C$, 9wt% carbon black and 6wt% styrene butadiene rubber (Hydrophilic binder LHB-108P, LICO Technology Corp) as binder. For preparation of suspensions, appropriate amounts of solvent, binder and carbon black were first mixed and impeller stirred. After one hour $LiFePO_4/C$ was added and the suspension stirred for additional 2 hours before tape casting took place. The solid weight percent for water and NMP system suspensions were 55% and 27%, respectively.

Tape casting with 80 μm gap was carried out by slowly moving the casting station with suspension manually over the aluminum foil. After drying in ambient conditions, casted cathode material with a thickness in the range of 60-80 μm were cut into 16 mm circular samples and pressed with 500 kN at 70°C for 30 seconds. Then the samples were further dried at 120°C for 12 hours and transferred to an argon filled glove box for storage until cell assembling took place.

3.8 Cell assembling and charge cycling test

The electrochemical properties of the produced powder materials were investigated by using two-electrodes, laboratory made cells. The $LiFePO_4$ cells were assembled in an argon filled glove box using lithium metal as anode and a separator membrane from Celgard (Trilayer PP/PE/PP separator, thickness 25 μm). The electrolyte was 1M $LiPF_6$ in a 1:1 wt% mixture of ethylene carbonate and diethyl carbonate (EC/DEC). Figure 8 shows a laboratory made $LiFePO_4$ cell prepared for cycling test.

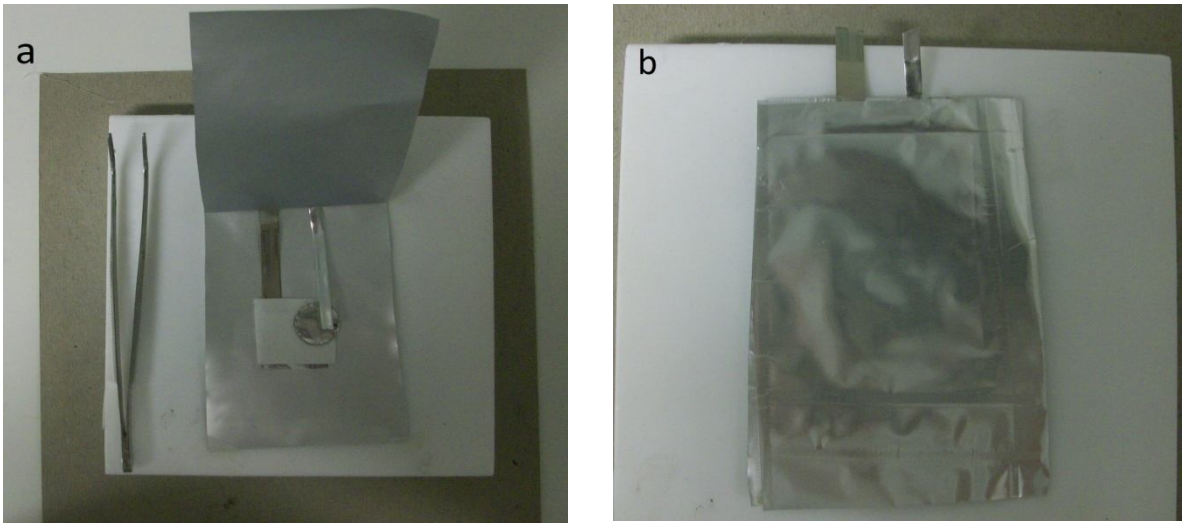

Fig 8. Illustration of a laboratory made $LiFePO_4$ cell. (a) Not completely sealed with cathode coated on Al circular foil and anode under the membrane. (b) Sealed cell ready for cycling test.

The galvanostatic charge and discharge characteristics of the cathodes were evaluated with galvanostatic cycling at room temperature between 2.7 and 4.2 V at the current rates 0.1 and 1 C. The sampling rate was 120 points/hour. C-rate expresses the charge or discharge current rates, in amperes, in multiples of the rated capacity. For example one gram $LiFePO_4$ active material rated at 170mAh provides 170mA for one hour if discharged at 1C rate. The same material discharged at 0.1C provides 17mA for ten hours [28].

The cycling results were represented in potential (V) vs. time (h), capacity (mAh/g) vs. cycle numbers and potential (V) vs. capacity (mAh/g) diagrams.

4. Results and discussion

4.1 Suspension preparation and freeze granulation

After completed mixing and ball milling of Li_2CO_3 and $FeC_2O_4*2H_2O$ with the first precursor combination, appropriate amount of $(NH_4)_2HPO_4$ aqueous solution was added to the mixture during stirring. Ball milling was intended to reduce particle size and increase the surface area. The ball milled mixture had still a low viscosity but after adding half of the $(NH_4)_2HPO_4$ aqueous solution the suspension viscosity suddenly increased accompanied by a gas producing reaction. Reactive surfaces of the mixed powders were exposed by the ball milling process and caused significantly increased speed of reaction. The high suspension viscosity trapped the produced gases and made further mixing and stirring difficult. Therefore, a significant dilution had to be conducted in order to enable addition of all required $(NH_4)_2HPO_4$ and obtain a reasonable viscosity level at the end, suitable for freeze granulation.

By using $NH_4H_2PO_4$ aqueous solution instead of $(NH_4)_2HPO_4$ in the second combination, the suspension thickening problem was less critical. However, adding $NH_4H_2PO_4$ to $Li_2CO_3/FeC_2O_4*2H_2O$ ball milled mixture was still accompanied by a reaction which produced gases and also caused a small increase in viscosity but it was acceptable for freeze granulation without any need of dilution.

Processing of the third precursor combination caused much less reaction and an appropriate viscosity level for freeze granulation was obtained without any dilution or extra conditioning time.

After addition of PVA, freeze granulation was conducted with all precursor suspensions without any problem and after freeze drying the granule batches were sieved and stored.

4.2 Calcination

Figure 9 shows the weight loss of the first precursor combination with 5% PVA during the calcination process, measured by the inbuilt balance of the furnace. There is an initial weight loss at temperatures below 180°C which can be attributed to the evaporation of physically absorbed water together with decomposition of lattice water from $FeC_2O_4*2H_2O$. It has been reported that pyrolysis of PVA occurs at 300-425 °C and only a small amount of residue survives at temperatures up to 450°C [23]. The weight loss in the temperature range of 180-450°C corresponds to rapid pyrolysis and decomposition of PVA together with decomposition of FeC_2O_4 and $(NH_4)_2HPO_4$ and the reaction between decomposed materials in order to produce crystalline $LiFePO_4$. The slight weight loss at temperatures higher than 450°C can be attributed to more decomposition of remaining PVA. The error in weight loss (weight gain) after 800°C (fig.9c.) can attribute to the thermocouple wire which fell on the balance due to the high degree of expansion at the calcination temperature. The weight loss pattern also shows

that pyrolysis of PVA and formation of $LiFePO_4$ occurred in the same temperature range. This indicates the possibility of creating a carbon coating with PVA during the calcination process.

a.

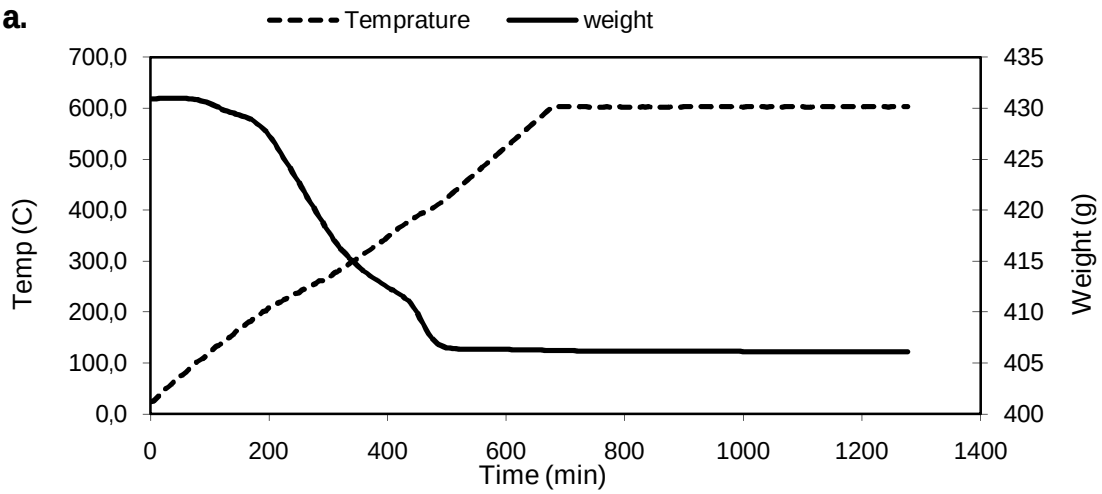

b.

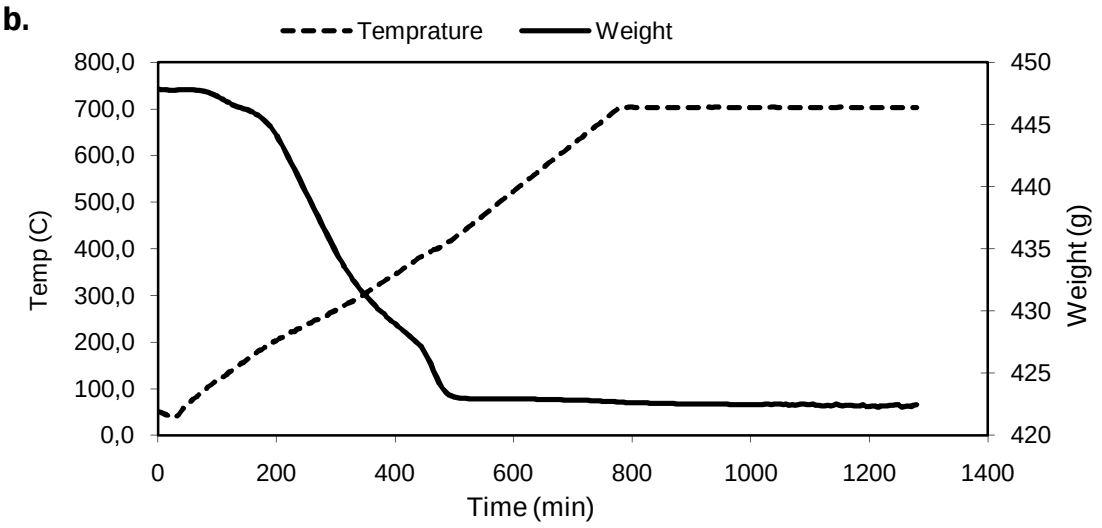

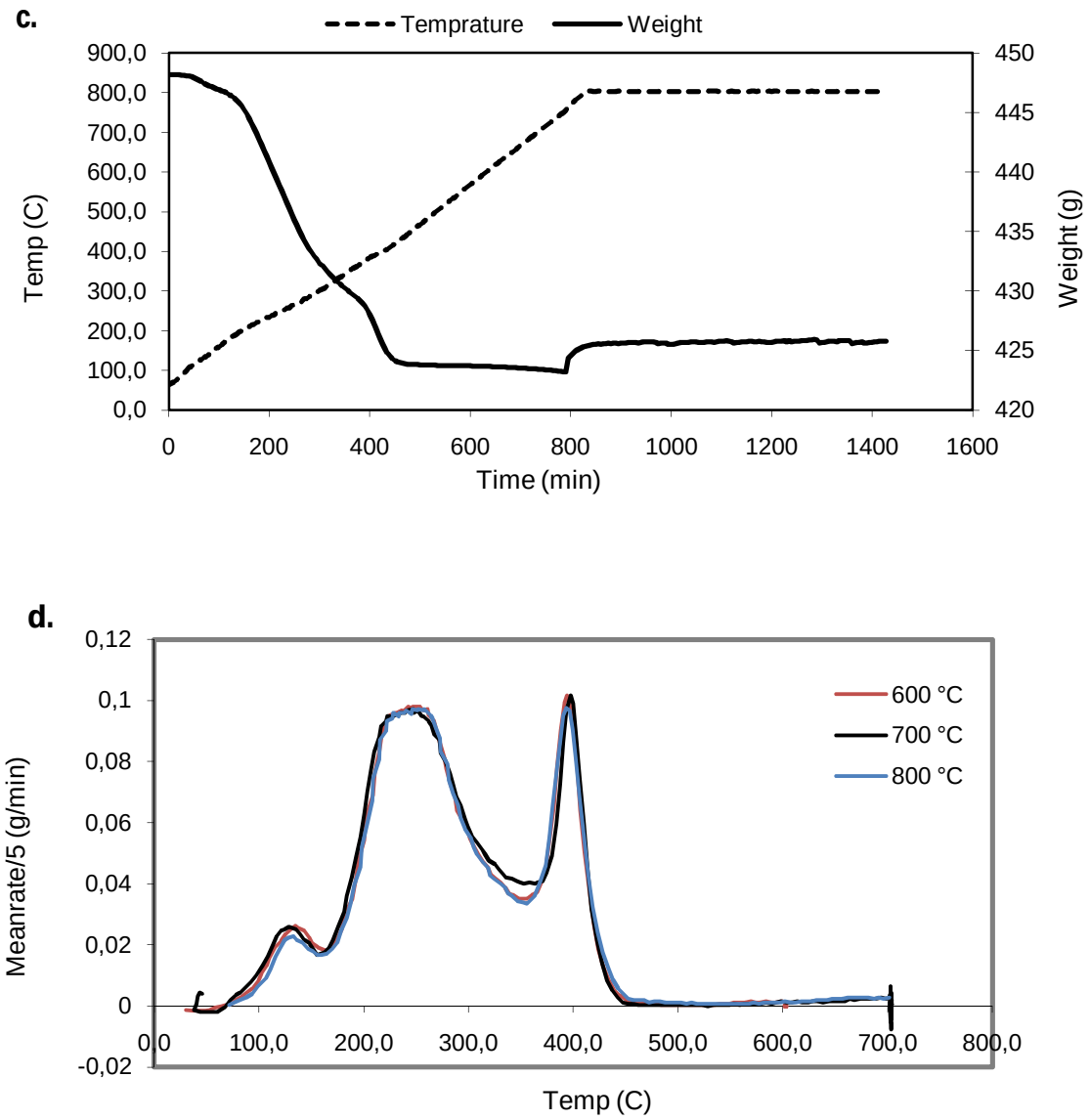

Fig. 9. Weight loss and temperature curves of first precursor combination with PVA at calcination temperatures of (a) 600 °C; (b) 700 °C; (c) 800 °C. (d) Rate of weight loss during calcination temperatures at 600, 700 and 800 °C.

For the first PVA containing precursor combination, the weight loss during calcination was in the range of 50-54% and for the second and third precursor combination it was 49-52% and 37-55%, respectively depending on the PVA content and calcination temperature. The greater the amount of PVA, the greater the amount of material available for decomposition will be and the greater weight loss during calcination can be expected. Higher temperature might also give a risk for decomposition of $LiFePO_4$ into other compounds that might result in weight loss. Therefore, besides a general coarsening of the material, it is essential to find an optimum (limited) calcination temperature.

4.3 Evaluation

The XRD analysis was conducted on several produced $LiFePO_4/C$ powders, $LiFePO_4$ powder that was synthesized without PVA with the first precursor combination and the commercial powder A. The resulting X-ray diffraction patterns are shown in figure 10 and appendix A. The impurity phases can be seen in all the XRD figures except figure 10 (d.) which is related to $LiFePO_4/C$ produced from the second precursor combination calcined at 700°C in Ar+10%H_2 atmosphere. All the diffraction peaks in figure 10 (d.) can be indexed on the orthorhombic structure with the space group Pnmb (indicated in red) and there are no impurity phase peaks. Although, the amounts of impurity phase peaks vary among the materials, it can be observed from the X-ray results that the third precursor combination contained more impurity peaks. The commercial powder A (fig.10. a.) and the powder without PVA (fig.10. f.) also have minor amount of impurities. The impurity phases can be iron (II or III) pyrophosphates or phosphates, perhaps $Li_3Fe_2(PO_4)_3$ or Li_3PO_4 [24]. In general, in every precursor combination, impurity peaks increase at higher calcination temperatures and they decrease by changing the calcination atmosphere from inert nitrogen to reductive argon + 10% hydrogen. Reductive atmosphere increases the purity by prohibiting the oxidation of iron from Fe^{+2} to Fe^{+3} and avoiding the consequent production of Fe^{+3} compounds. It should be emphasized that evaluation of the XRD results, regarding presence of impurities, does not give a quantification but only lead to the conclusion that they exist or not in minor or major quantities. There are no additional peaks associated with the crystalline carbon (graphite) in the diffraction patterns, which indicates that the carbon generated from PVA is amorphous and its presence appears to not affect the structure of $LiFePO_4$.

It is found that the average X-ray patterns of $LiFePO_4$ made from the second and third precursor combination have the strongest and weakest relative intensity, respectively. Besides, the intensity of peaks in first and second precursor combination are stronger than the commercial powder A. By increasing calcination temperature in each precursor combination the sharpness and intensity of the peaks increase which indicates an increase of crystallinity that may occur supported by a growth of grain size, ordering of local structure and release of lattice strain [24]. The $LiFePO_4/C$ powder which showed the highest purity (fig.10. h.) had has also high relative intensity peaks that made it to a promising powder for the further cathode production, cell assembling and cycling test.

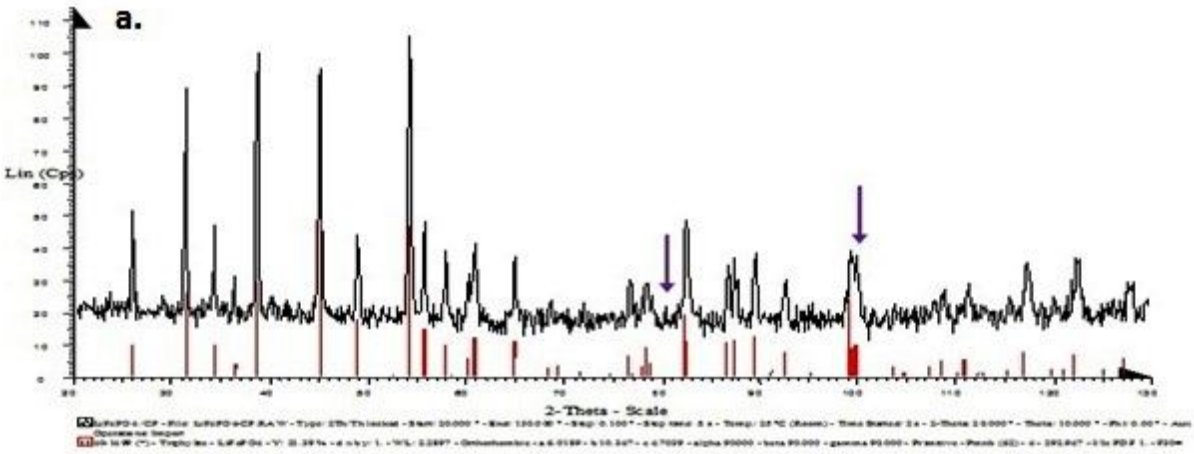

a) Commercial $LiFePO_4/C$ powder A

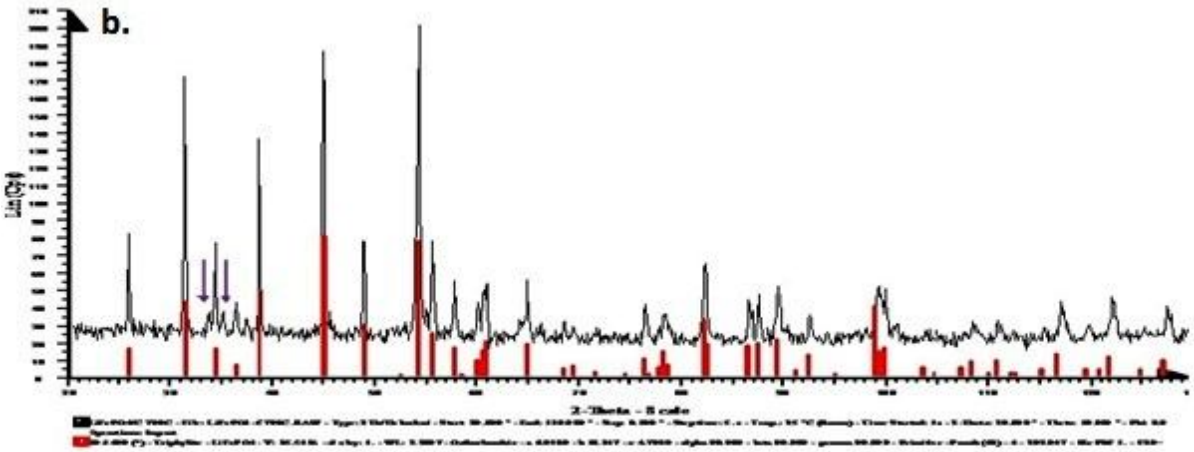

b) b. $LiFePO_4/C$, first precursor combination,700°C&10h, 5% PVA , N_2

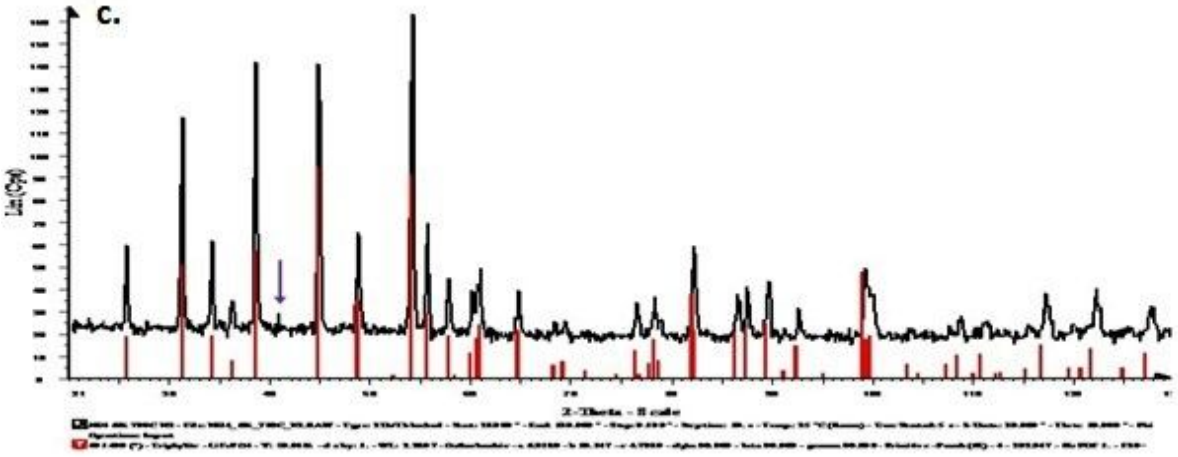

c) f. $LiFePO_4/C$, second precursor combination,700°C&10h, 6% PVA , N_2

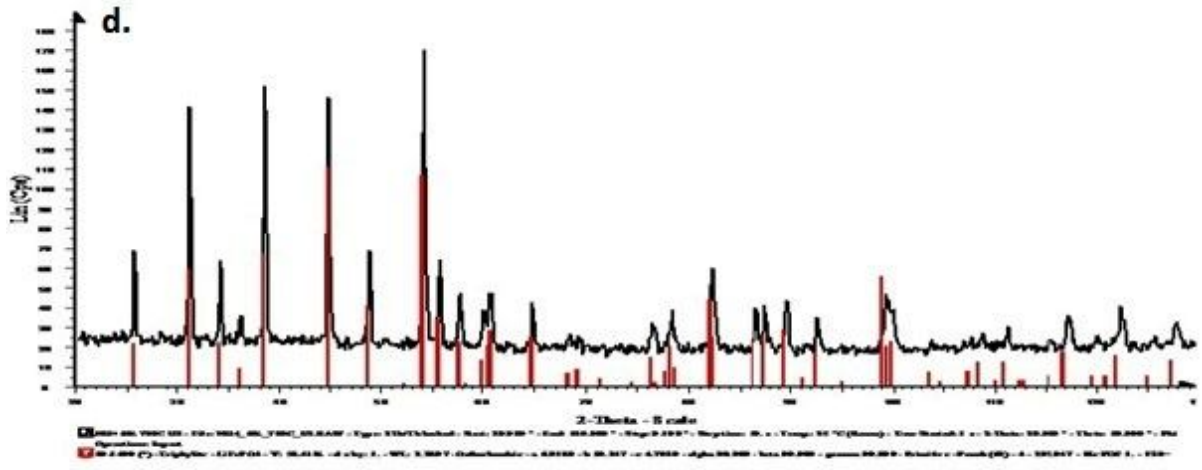

d) h. $LiFePO_4/C$, second precursor combination,700°C&10h, 6% PVA ,Ar+10% H_2

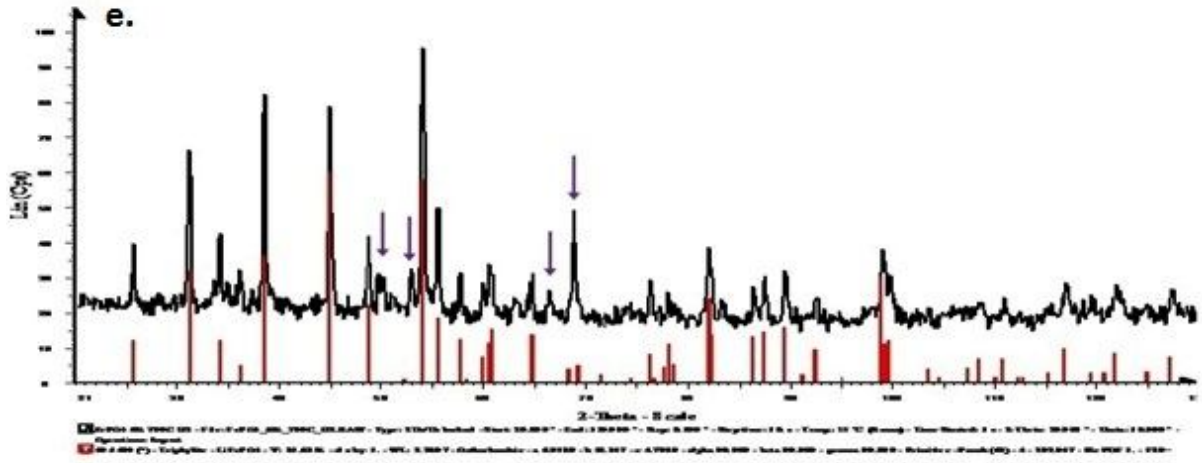

e) n. $LiFePO_4/C$, third precursor combination,700°C&10h, 6% PVA ,Ar+10%H_2

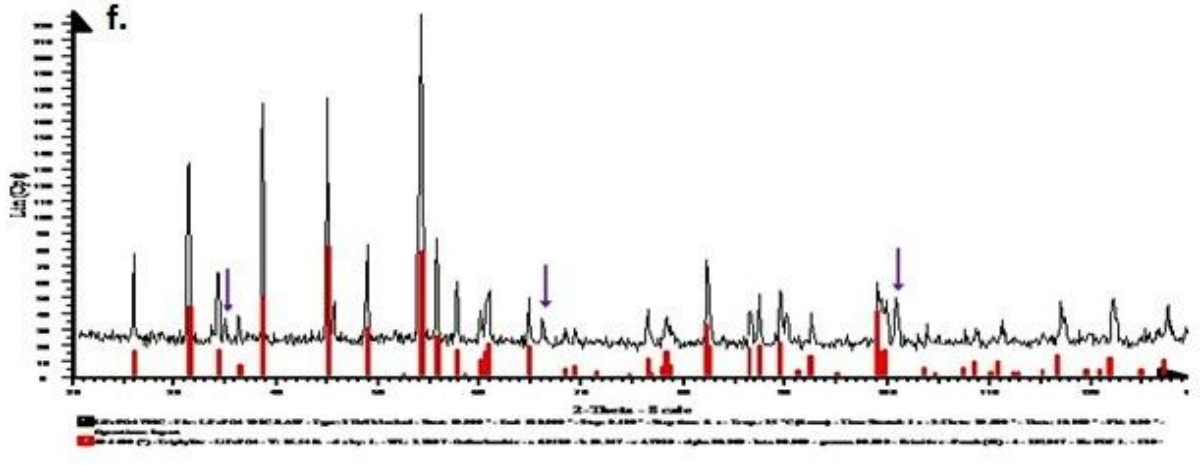

f) $LiFePO_4$, first precursor combination,700°C&10h, No-PVA , N_2

Fig. 10. XRD spectra of: (a.) commercial $LiFePO_4/C$ powder A, (b.) -(e.) $LiFePO_4/C$ produced from first, second and third precursor combination calcined at 700°C, (f.) $LiFePO_4$ produced from first precursor combination without PVA. The impurity peaks are marked with reverse arrows.

The morphology of the $LiFePO_4$ and $LiFePO_4/C$ powders which were synthesized from the first precursor combination are illustrated in figure 11. It can be observed that $LiFePO_4$ crystals are embedded in a porous structure of carbon caused by decomposition of PVA during the calcination. In general, the $LiFePO_4/C$ composites show a huge amount of independent nano-sized particles that are closely packed within a porous structure of carbon. It was found that the $LiFePO_4/C$ had smaller and rougher surface texture crystals than the corresponding $LiFePO_4$ sample. Further, as the calcination temperature increased, the crystal size increased more in the material without PVA than in the $LiFePO_4/C$ powders. Therefore, it can be concluded that the decomposition of the PVA to a porous carbon structure limited the growth of particles during the calcination. This phenomenon is caused by a carbon covering of the $LiFePO_4$ particles that inhibits grain growth by decreasing the diffusion rate of atoms.

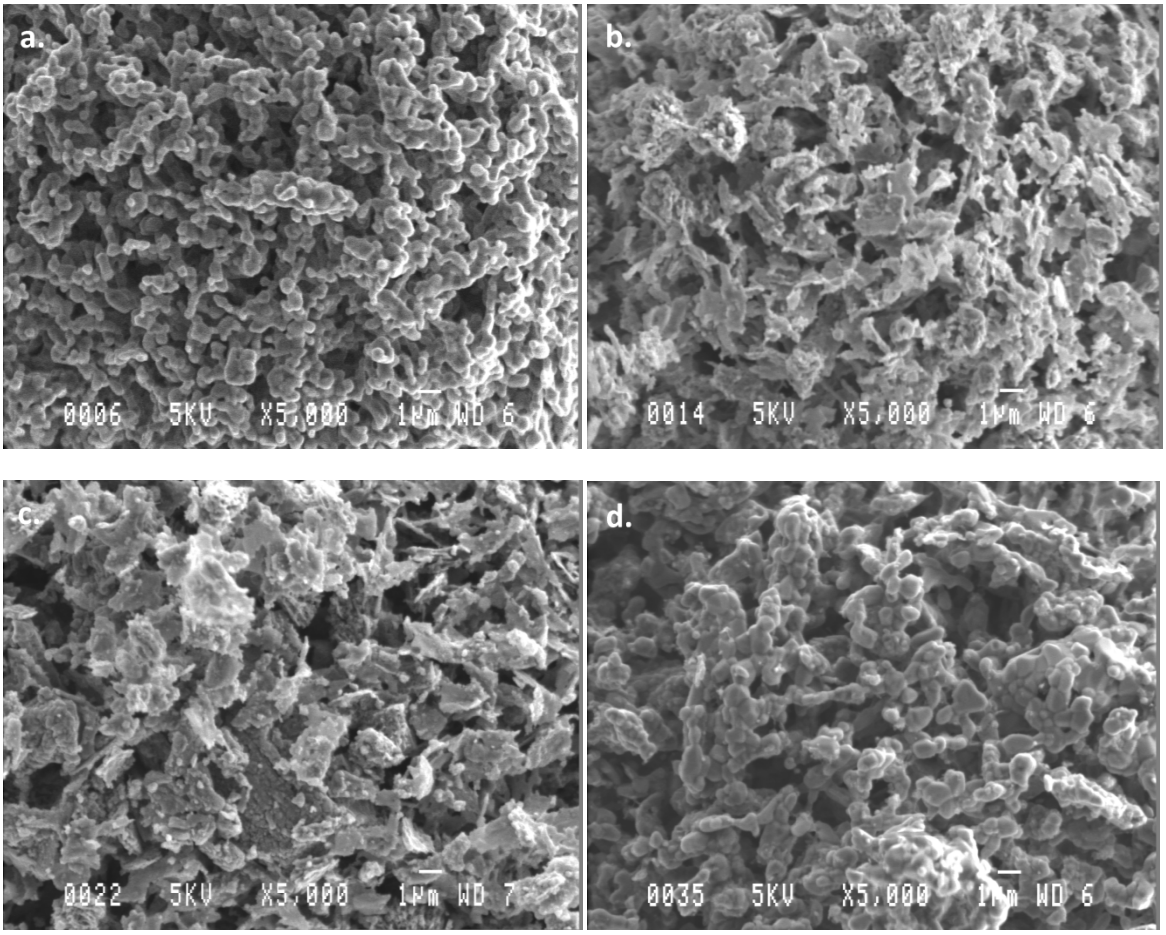

Fig 11. SEM morphology of samples synthesized from first precursor combination prepared at different temperatures (a.) $LiFePO_4$ at 700°C; (b.)-(d.) $LiFePO_4/C$ at 600, 700, 800°C, respectively.

Elemental maps of carbon, iron, oxygen and phosphorus of $LiFePO_4/C$ synthesized from first precursor combination at 700°C are shown in figure 12 (a.) to (d.). It is clear that the produced $LiFePO_4$ has a high homogeneity and the elements are well distributed in the powder. Thus, the conductivity of $LiFePO_4/C$ compounds would be enhanced due to uniform distribution of $LiFePO_4$ crystals in a homogenous carbon web (network).

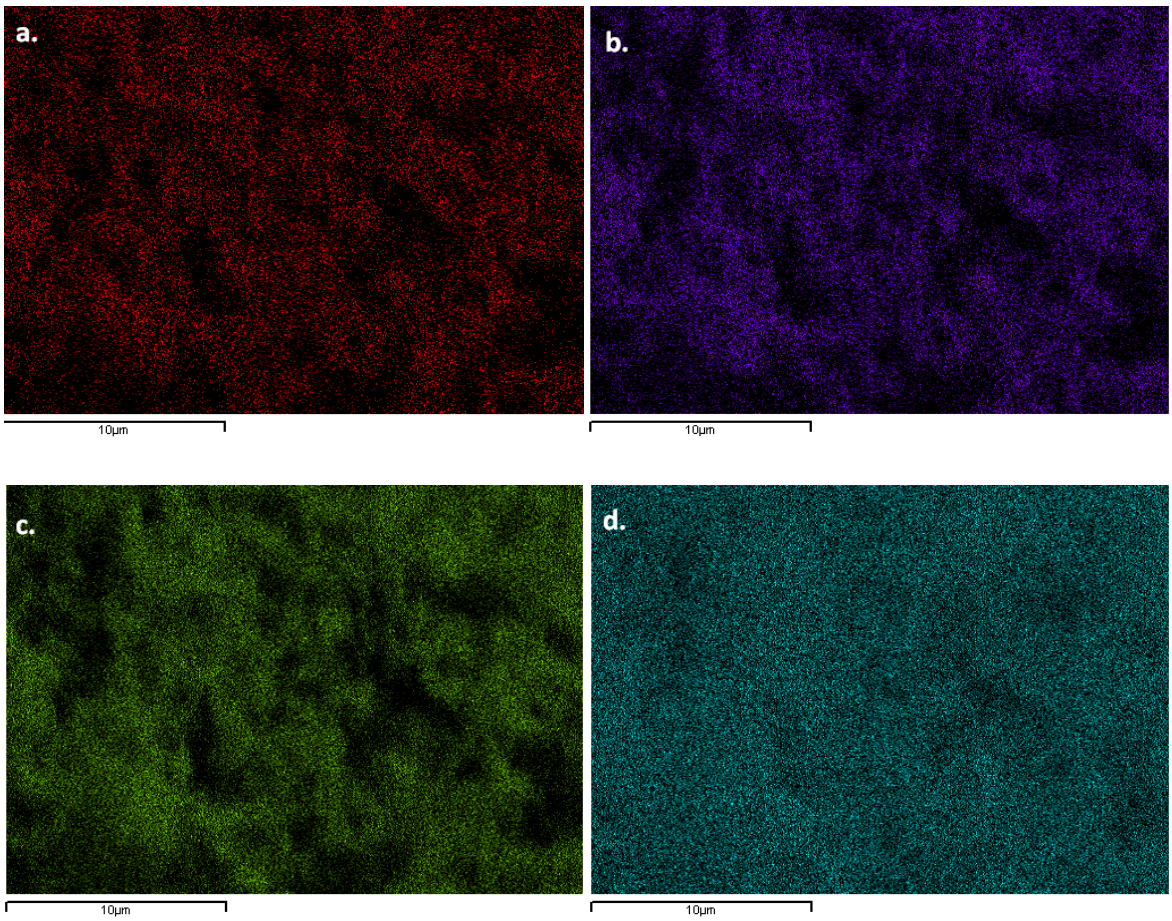

Fig. 12. Elemental map of $LiFePO_4/C$ calcined at 700°C; (a.) carbon; (b.) iron; (c.) oxygen and (d.) phosphorus.

Table 9 shows data from measurements of density, carbon content and conductivity of prepared $LiFePO_4/C$ and commercial powders. As it exists certain complications (described below) and error margins, the measured data should be taken as indicative trends and guiding for the material choice for battery cell application.

$LiFePO_4$ with a close-packed oxygen array in the ordered olivine structure provides an effective volume utilization with a theoretical density of 3.6 g/cm^3 [2]. Normally, increasing the residual carbon of $LiFePO_4/C$ causes a decreas in its density. The density measurement results from prepared $LiFePO_4/C$ vary between 3.3-4.2 g/cm^3. The variations should be related to differences in the amount of PVA and calcination temperatures and resulting carbon residues. Also, closed porosities may exist that influenced the density measurement. More closed porosity leads to larger errors in the

density measurement and causes an underestimation of the density. Measured density of the commercial powder A and B was 4.0 and 3.4 g/cm^3, respectively.

Table 9. Powder density, tablet conductivity and residual carbon content of commercial and prepared $LiFePO_4/C$ powders.

Precursor group	Calcination temp. and atmosphere	PVA%	Density (g/cm^3)	Conductivity (S·m^{-1})	Carbon content (wt%)
(I)	600°C , N2	5	3.3	0.0078	3.16
(I)	700°C , N2	5	4.0	0	1.04
(I)	800°C , N2	5	4.2	0.000005	0.4
(II)	650°C , N2	5	3.9	0.1	
(II)	650°C , N2	6	3.9	0.16	
(II)	650°C , N2	7	4.1	0.2	
(II)	700°C , N2	5	4.1	0.03	2.22
(II)	700°C , N2	6	3.8	0.13	2.88
(II)	700°C , N2	7	4.0	0.26	3.14
(II)	700°C, Ar+10%H2	5	4.4	0.39	2.77
(II)	700°C, Ar+10%H2	6	3.4	0.47	3.24
(II)	700°C, Ar+10%H2	7	3.4	1.65	3.61
(II)	750°C, N2	5	4.2	0.000003	
(II)	750°C, N2	6	4.0	0.0018	
(II)	750°C, N2	7	3.9	0.0027	2.35
(III)	650°C , N2	5	3.3	0.13	
(III)	650°C , N2	6	3.4	1.14	
(III)	650°C , N2	7	3.8	1.78	2.69
(III)	700°C , N2	5	4.0	0	
(III)	700°C , N2	6	4.1	0.014	
(III)	700°C , N2	7	4.0	0.18	1.12
(III)	700°C, Ar+10%H2	5	3.4	2.29	
(III)	700°C, Ar+10%H2	6	4.1	6.07	
(III)	700°C, Ar+10%H2	7	4.2	8.2	2.81
(III)	750°C, N2	5	3.8	0	
(III)	750°C, N2	6	3.8	0	
(III)	750°C, N2	7	3.6	0	
commercial powder A			4	2.39	1.73
commercial powder B			3.4		4.31

Carbon plays three beneficial roles during synthesis of the $LiFePO_4/C$: 1) as a reducing agent to avoid formation of ferric phases, 2) to block the inter-particle contact and hinder the undesirable grain growth during calcination, and 3) to enhance the electronic conductivity of material. However, carbon adversely affects the density of active

material. Therefore, the $LiFePO_4/C$ composite should be prepared with the minimum carbon content required for getting sufficient conductivity of the composite material.

Carbon content measurement was done on several prepared $LiFePO_4/C$ materials as well as commercial powders, as shown in table 9. The selection of powders was done in order to get a reasonable comparison using a minor amount of tests. Figure 12 shows the results of the second precursor combination and illustrates the effect of PVA content, calcination temperature and atmosphere on the residual carbon in the $LiFePO_4/C$ powders. It is clear that the residual carbon increased as the PVA content increased and decreased as the calcination temperature increased. Carbon can react with present oxygen in the material at higher temperatures and expel as carbon oxides and it can also decompose the $LiFePO_4$ into other phases. The results from $Ar+10\%H_2$ atmosphere at 700°C show higher residual carbon than the similar one in nitrogen atmosphere, which is due to the more reductive environment with hydrogen.. The effect of the mentioned parameters on the carbon residues are illustrated in figure 12 and are in agreement with the other obtained results (density and conductivity) presented in table 9.

The $LiFePO_4/C$ powder which was produced from the second precursor combination and calcined at 700°C in $Ar+10\%H_2$ atmosphere showed the highest carbon content (3.61%) with an acceptable density of 3.4 g/cm^3. These facts together with an accurate phase composition showed by the XRD, so far made it the most favorable choice as active material for cathode production.

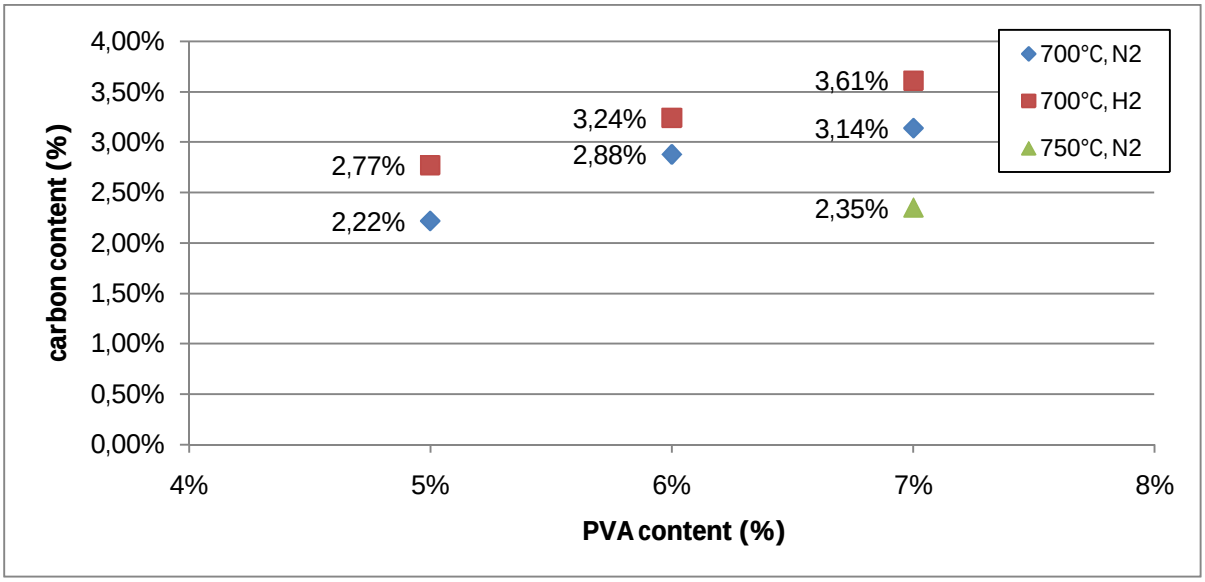

Fig. 12. Effect of PVA, calcination temperature and atmosphere on residual carbon of $LiFePO_4/C$ synthesized from second precursor combination.

$LiFePO_4$ is reported to be almost an insulator with electronic conductivity of $< 10^{-9} Scm^{-1}$ [2]. However, as a cathode material has to be a mixed ionic-electronic conductor. It is

essential to add a conductive material such as carbon to enhance the conductivity of $LiFePO_4$ to a great extension. Conductivity data of produced $LiFePO_4/C$ powders and commercial powder A are shown in table 9. The data is based on an average value for two tablets of each material with the maximum difference of 0.08 $S.m^{-1}$. It was not possible to make tablets from commercial powder B due to weak adhesion of the powder particles at pressing. Produced tablets from the different precursor combinations had different tablet density. Tablets from the third precursor combination had higher density (1.94-2.24 g/cm^3) in comparison to the first and second combinations (1.8-2 g/cm^3), whereas the commercial powder A had the highest tablet density of 2.25 g/cm^3. The higher tablet density is most probably related to the higher packing and less amount of porosity. A complication for an adequate valuation of the conductivity vs tablet porosity is, however, the uncertainty in powder density measurement and possible closed porosity of the powder. The conductivity results showed that the higher carbon content in a specific group of precursor combination the higher conductivity was obtained. $LiFePO_4/C$ powders prepared from the third precursor combination calcined at 700°C in Ar+10%H_2 atmosphere showed the highest conductivity. This can be referred to the high carbon content and less tablet porosity or possibly the existence of more conductive impurity phases in this material.

It is desirable to compensate the low conductivity by using active material in form of very small sized particles in order to decrease the diffusion length of the Li^+ ions and thus manage the problem with slow diffusion in the material. Resulted active material with higher surface area has larger number of reaction sites, which enhance the material utilization. Moreover, smaller particles have lower effective volume change during insertion/extraction of Li^+ ions which leads to better structural integrity properties during charging and discharging. On the other hand it might be harder to process a powder with very high surface in terms of preparation for casting of cathode layers. Normally, a powder with high surface area is also more difficult to pack densely, which influences the cell performance in terms of available active $LiFePO_4$ per volume unit cathode material.

The specific surface area of the prepared $LiFePO_4/C$ samples is shown in figure 13. Figure 13 (a) illustrates the effect of calcination temperature on the specific surface area of the first precursor combination. As expected, the specific surface area decreases as the calcination temperature increase showing more grain growth that occurs at higher temperatures. Figure 13 (b) and (c) shows the effect of carbon content (in terms of percentage amount of PVA) and calcination atmosphere on the specific surface area for the second and third precursor combination, respectively. The results confirm the mentioned effect of calcination temperature on the specific surface area and also indicate that the specific surface area increases by increasing the amount of PVA. This is most probably due to the exictance of more residual carbon that inhibit the grain growth, but the carbon might also contribute to the surface area itself. The results also indicate that the $LiFePO_4/C$ powders calcined in reductive atmosphere of Ar+10%H_2 have higher surface area than the corresponding powders in N_2 at the same

temperature. Reductive atmosphere also causes more residual carbon that inhibits the grain growth.

The specific surface area of the commercial powders A and B was measured to 14.1 and 35.9 m^2/g, respectively. In general, the third precursor combination showed lower surface area in comparison to the first and second one. The $LiFePO_4/C$ powders based on second precursor group, produced at 700°C in Ar+10%H_2 atmosphere possess the highest specific surface area considered positive with respect to available exposition for Li-ions. Additionally, characterized by the best conductivity of all produced materials, excluding group three, made this to the most promising candidate as active cathode material. Still, the surface area was not extreme and considered suitable for the processing in cathode manufacture.

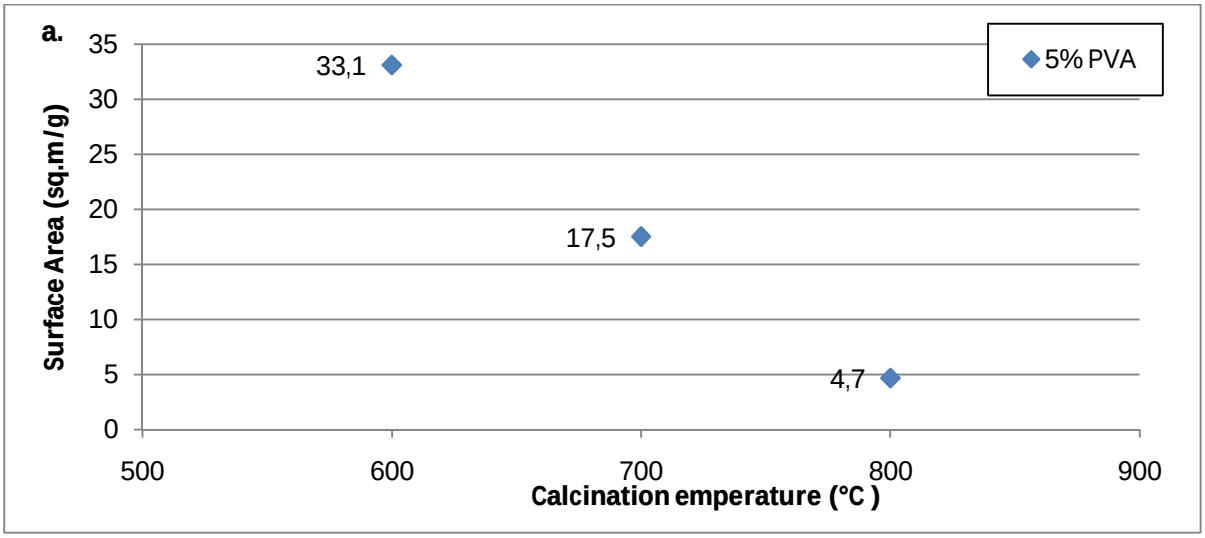

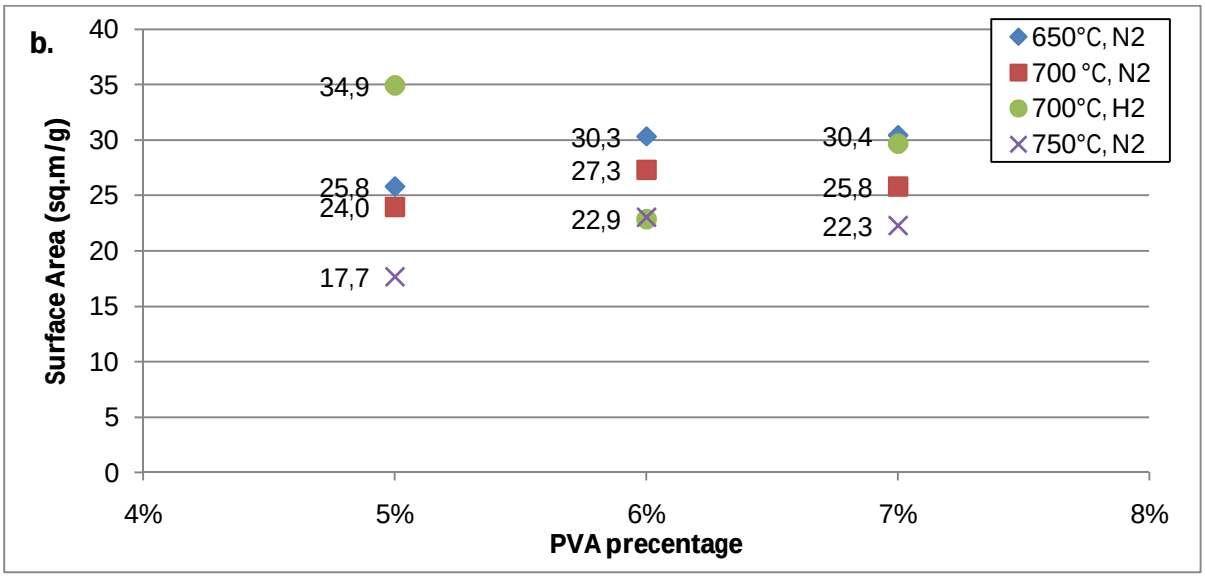

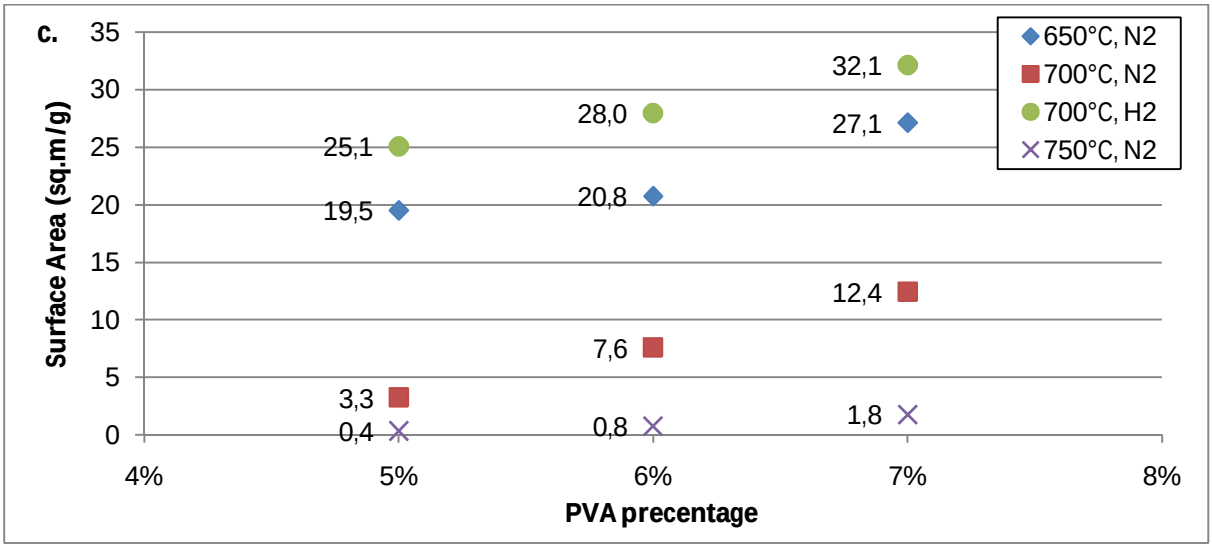

Fig. 13. Specific surface area of $LiFePO_4/C$ powders; (a.) effect of temperature on specific surface area of first precursers combination; (b.) and (c.) effect of temperature, PVA percent and calcination atmosphere on specific surface area of second and third precurser combination,respectively.

To summarize, the results confirm that the optimal $LiFePO_4/C$ powder for cell production was the one synthesized by utilizing the second precursor combination with 7%PVA and calcined at 700°C in Ar+10%H_2. The mentioned powder did not only possess the highest purity (according to the XRD results) and high carbon content of 3.61%, its specific surface area was also in a suitably high level of 29.6 m^2/g and its density was 3.4 g/cm^3, which is close to the theoretical density of $LiFePO_4$. Although, this sample shows a comparative low electrical conductivity of 1.65 $S.m^{-1}$ versus the commercial powder A it was considered acceptable due to the other advantages. Accordingly, it was decided to use this $LiFePO_4/C$ powder as the active material in cathode production and cell assembly.

4.4 Paste fabrication, tape casting and cell assembling

With the pre-milled/FG-processed selected powder, pastes were prepared using solvent (NMP) or water as liquid medium. Due to previous experiences at Swerea IVF it was decided to use 85 wt% active material ($LiFePO_4/C$), 9wt% carbon black and 6wt% styrene butadiene rubber binder in the water based system to obtain suitable paste properties. However, for the NMP based pastes 80 and 90 wt% active material, respectively, 5 and 10 wt% carbon black and 5 and 10 wt% PVDF binder were used according to common compositions presented in literature. It was observed that larger volume of NMP compared to water was required to wet all the solids and reach an acceptable viscosity for tape casting. For example 45wt% water was used for water based paste whereas 63 and 72 wt% NMP was used for 90 and 80wt% active material NMP based pastes, respectively. Since the NMP solvent is toxic and required in large volumes, replacing it with water is obviously a great benefit for the environmental concerns.

Manual tape casting was used to prepare the cathode material as it allows processing of small paste quantities. The disadvantage is that it is difficult to obtain constant casting condition in terms of speed and pressure on the cast station. This will result in an uneven layer thickness and variation in the smoothness. It was observed that the NMP based casted cathode with 90% active material had very weak adhesion to the substrate foil after drying. The weak adhesion was caused by insufficient amount of PVDF as binder and higher concentration of active material in the suspension paste. It was not possible to use the mentioned casted cathodes for cell production due to the easy separation of the cathode material from the aluminum foil substrate. Therefore, it was decided to conduct cell assembling with the two remaining produced cathode materials. Figure 14 presents tape casted cathode materials on an aluminum foil prior to cell fabrication process.

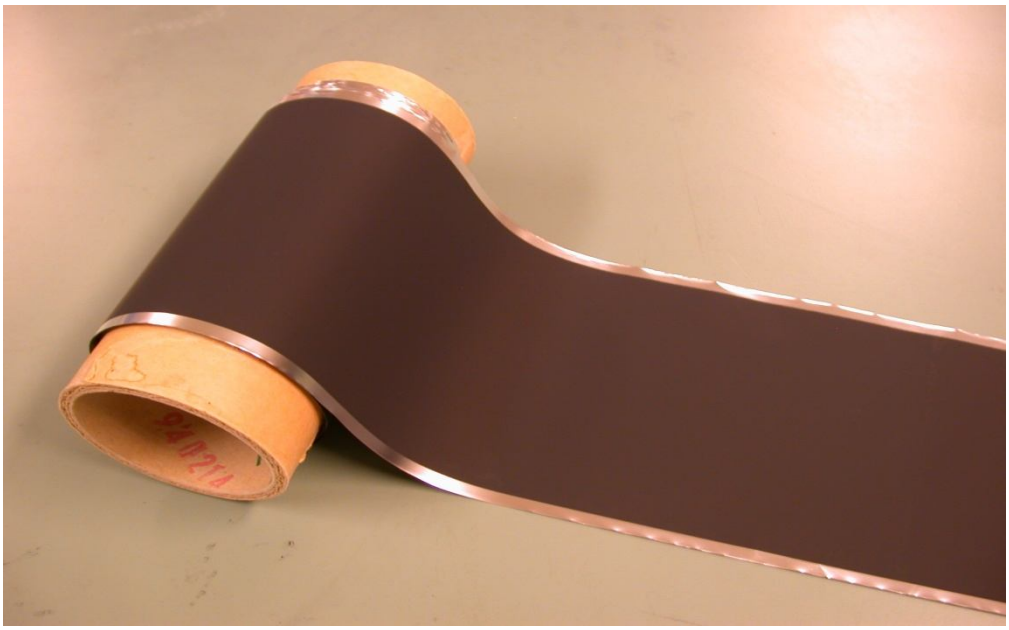

Fig. 14. Illustration of a tape casted cathode material on an aluminum foil prior to the cell fabrication process.

4.5 Charge-recharge test

The following equations express the charge (extraction of lithium) and discharge (insertion of lithium) of the $LiFePO_4$ cathode. The charge-recharge equations of $LiFePO_4$ cathode are based on lithium containing and lithium free phase reactions [2].

- $LiFePO_4 - xLi^+ - xe^- \longrightarrow xFePO_4 + (1-x)\ LiFePO_4$ (charging)
- $FePO_4 + xLi^+ + xe^- \longrightarrow xLiFePO_4 + (1-x)FePO_4$ (discharging)

The charging and discharging of the $Li/LiFePO_4$ cell occurs at about 3.5 and 3.3 V, respectively. The reactions contain the insertion and extraction of lithium ion from Li_xFePO_4 over a large amount of x at a constant voltage independent of x [2]. This charge-discharge voltage pattern is one of the main characteristic of $LiFePO_4$.

The charge-discharge test was conducted on six prepared cells; three from water based and three from NMP based cathode fabrication. The cathodes prepared via water processing were labeled 1a, 1b and 1c and the cathodes prepared via solvent processing were labeled 2a, 2b and 2c. The loading factor of active material in sample 1a, 1b and 1c were 5.8, 3.9 and 3.9 mg/cm^2, respectively. For sample 2a, 2b and 2c the loading factors were 3.5, 3.1 and 2.6 mg/cm^2, respectively. The differences reflect the mentioned variation of layer thickness obtained by the manual casting. All the tests were performed directly after cell assembling as the cell package film showed a tendency to degrade after several days. The cell package film consists of a plastic film glued on an aluminum film. The electrolyte appeared to dissolve the glue and consequently the plastic film separated from the aluminum film after almost ten days. The aluminum film is necessary to protect the cell from oxygen and water vapor. Accordingly, when the aluminum film detaches and only the plastic film encloses the cell, the capacity might decrease due to the presence of oxygen and water vapor. However, the tests were done before such effect occurred. The cells were tested first at 0.1C rate for almost 5 days and then the current was changed to 1C rate for approximately one day to measure at least five charge-discharge cycles at each current rate.

Figure 15 shows the voltage vs. time curves of two of the prepared cells, samples 1c and 2c, representing the better results versus the others. Figures 15(e. and f.) and 15(g. and h.) belong to the 1c and 2c samples, respectively. The samples were tested at 0.1C (fig. 15.e. and 15.g.) and 1C (fig. 15.f. and 15.h.) current rates in the voltage range of 2.7-4.2V. The repeating patterns and flat plateaus at about 3.5 and 3.3 V exhibit the excellent reversibility during cycling. The flat plateaus are exactly at the same voltages as the theoretical two phase reactions happen in the electrodes (mentioned equations) which demonstrate the main characteristics and true electrochemical performance of the $LiFePO_4$ cells. The voltage vs. time curves of the all tested cells follow the same orders as it is in figure 15 except samples 1b at 1C current rate. The resulted curves for the mentioned sample were totally invalid in Li/ $LiFePO_4$ cell performance, so it was decided to not apply its results in the further investigation.

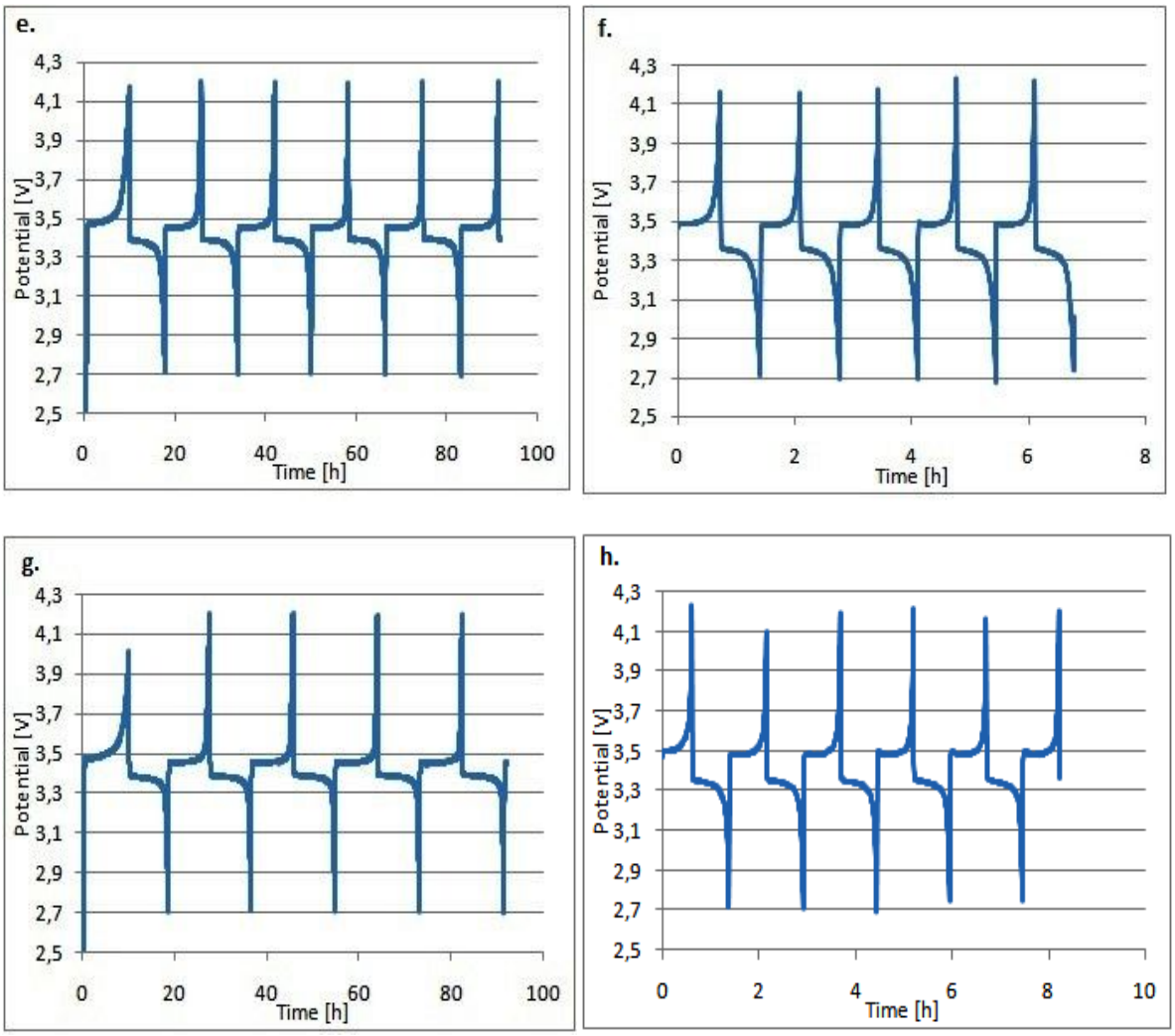

Fig. 15. Voltage curves during cyclic performance of samples 1c and 2c with $LiFePO_4$/C cathodes; (e.) and (f.) sample 1c at 0.1 and 1C, respectively; (g.) and (h.) sample 2c at 0.1 and 1C, respectively.

Figure 16 shows the comparison of the fifth charge-discharge voltage curves of the prepared cells. Figure 16 (e.) and (f.) belong to the cells with water based cathode preparation at 0.1C and 1C, respectively as well as figures (g.) and (h.) that belong to NMP based cathode preparation cells. A flat profile over a wide range around 3.5V for charging and 3.3V for discharging indicates an adequate extraction and insertion process of lithium ions between $FePO_4$ and $LiFePO_4$ in the cathode electrode.

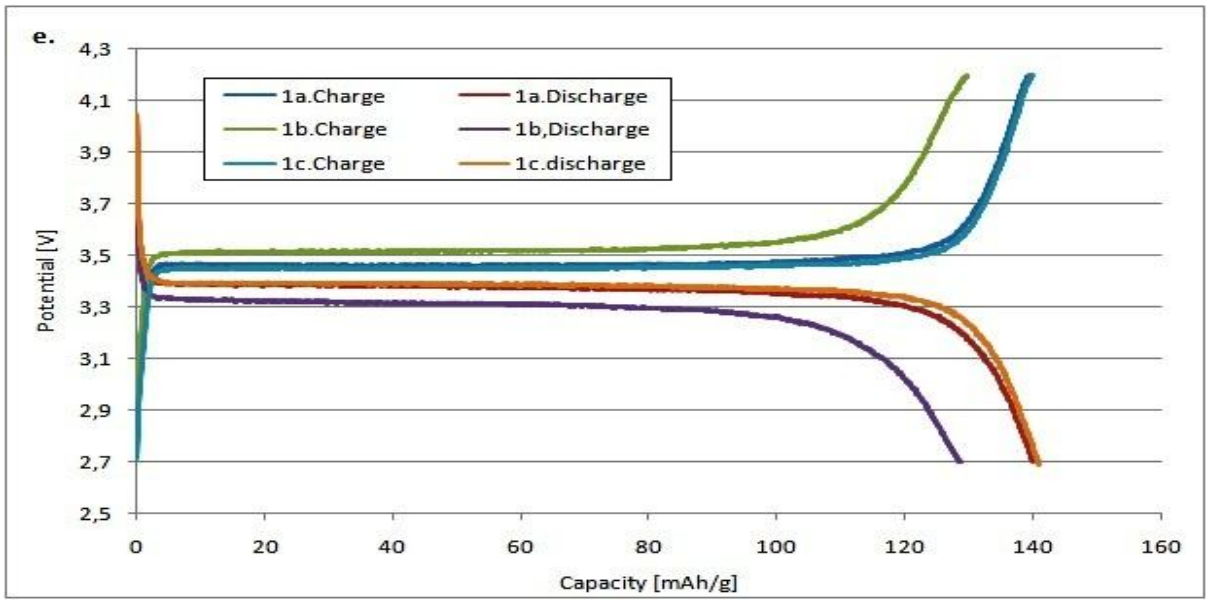
e.
1a.Charge
1a.Discharge
1b.Charge
1b,Discharge
1c.Charge
1c.discharge
Potential [V]
Capacity [mAh/g]

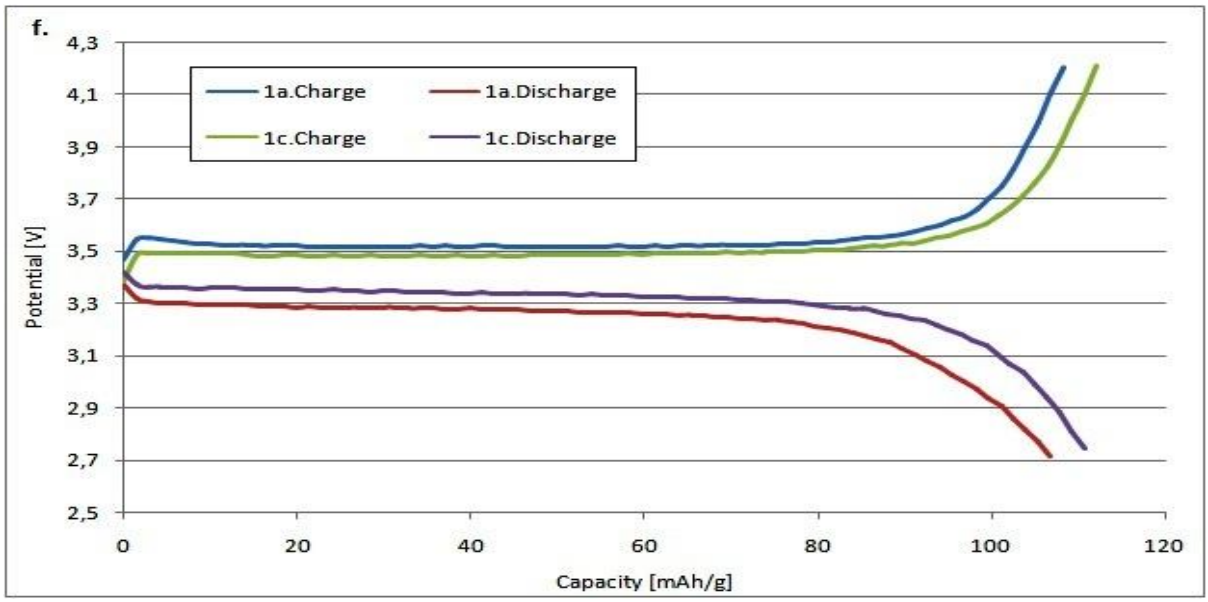
f.
1a.Charge
1a.Discharge
1c.Charge
1c.Discharge
Potential [V]
Capacity [mAh/g]

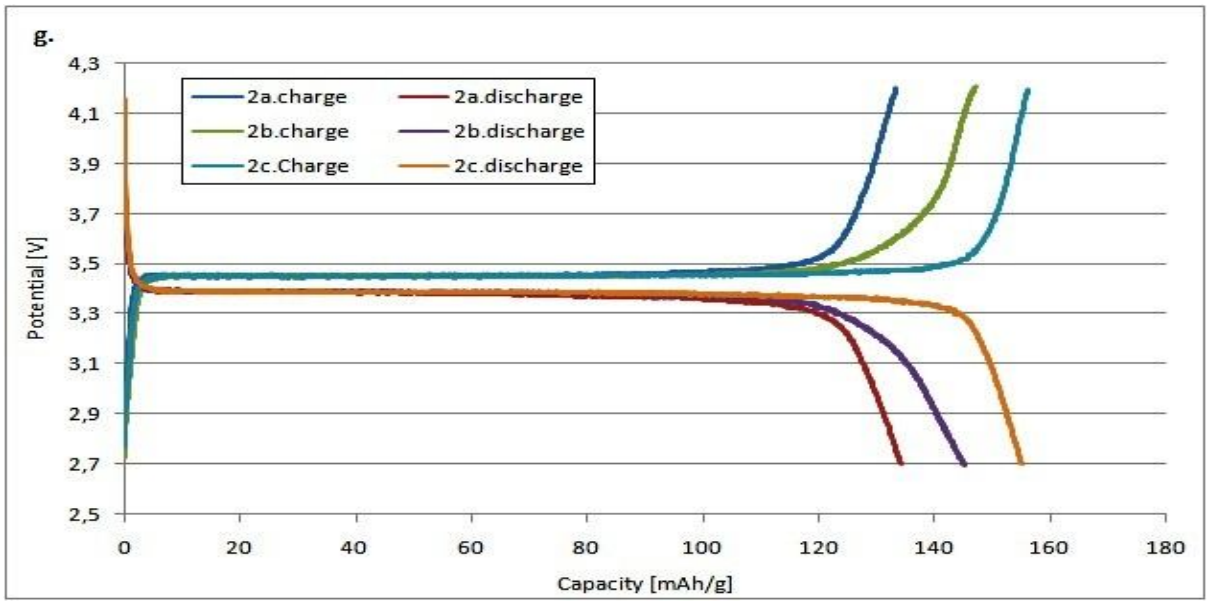
g.
2a.charge
2a.discharge
2b.charge
2b.discharge
2c.Charge
2c.discharge
Potential [V]
Capacity [mAh/g]

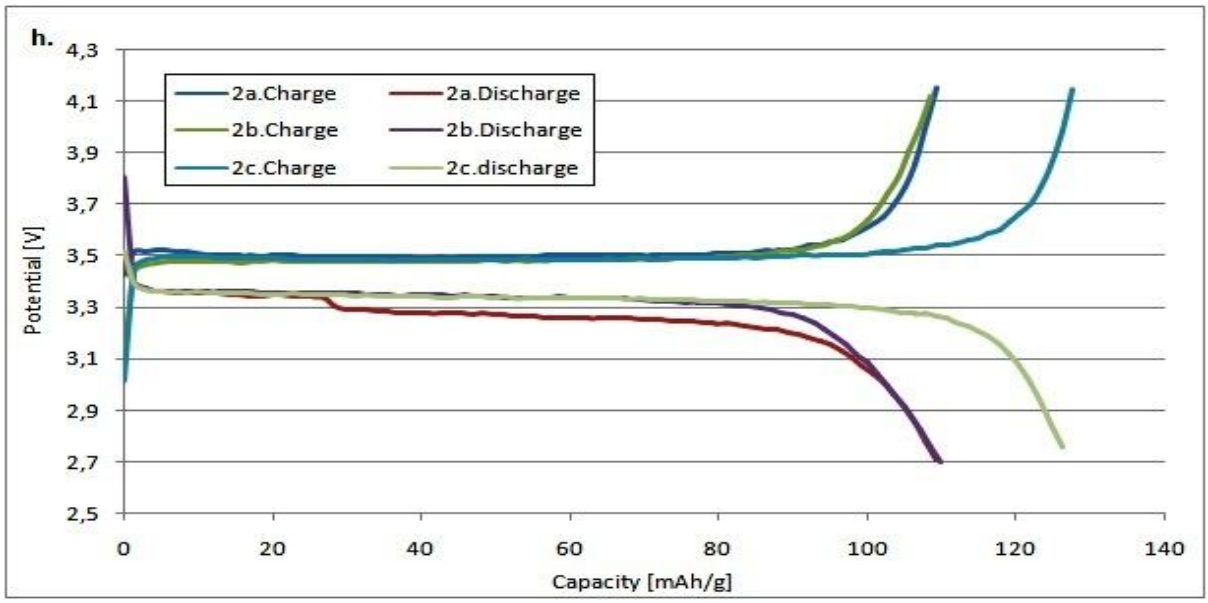

Fig. 16. Voltage profile on the fifth cycle of prepared cells for: (e.) and (f.) water base cathode preparation at 0.1C and 1C, respectively; (g.) and (h.) NMP base cathode preparation at 0.1C and 1C, respectively.

The specific capacity of all the prepared active materials are lower than the theoretical specific capacity of $LiFePO_4$ owing to the various factors such as intrinsic kinetic and conductivity limitation of the material, influence of cathode electrode additives and current density. The specific capacity of the samples at 0.1C rate is higher than their capacity at 1C. By increasing the current density, the discharge capacity and the plateau voltage is rapidly reduced due to the limitations of electronic and lithium-ion diffusion in the material. Samples named 1c and 2c have the highest specific charge-discharge capacity at the fifth cycle in their groups. The variation in specific capacity in each group might be caused by variations in cathode material thickness. It is reported that the electrochemical properties of cathodes are strongly influence by the cathode thickness [2]. If the porosity is the same, thinner electrodes deliver higher capacity than thicker ones due to lower electrode resistance and faster Li-ion conduction through the electrode. Sample 1c and 2c had the lowest loading factor that probably can conclude that they have the smallest thickness in their groups.

Figure 17 shows the quantity of the charge and discharge capacity of the tested cells at 0.1C (e.) and 1C (f.) rate. It is clear that the charge and discharge capacities are almost equal that indicates the excellent reversibility of $Li/LiFePO_4$ cells during cycling caused by the structural similarity of $LiFePO_4$ and $FePO_4$ [12]. Sample 1c showed the discharge capacity of 140 and 112 mAh/g at 0.1C and 1C current rate, respectively. On the other hand, sample 2c has the highest discharge capacity of 155 and 126 mAh/g at 0.1C and 1C rate, respectively, which correspond to 91% and 74% of the theoretical capacity of the olivine $LiFePO_4$. Although the amount of active material in sample 2c is lower than sample 1c, it showed higher capacity. The higher capacity of the sample 2c can be

attributed to the cathode composition and production method and its smaller thickness. In cathode production with water system a small residue of water vapor in samples can also affect the cell performance and significantly reduce the specific capacity.

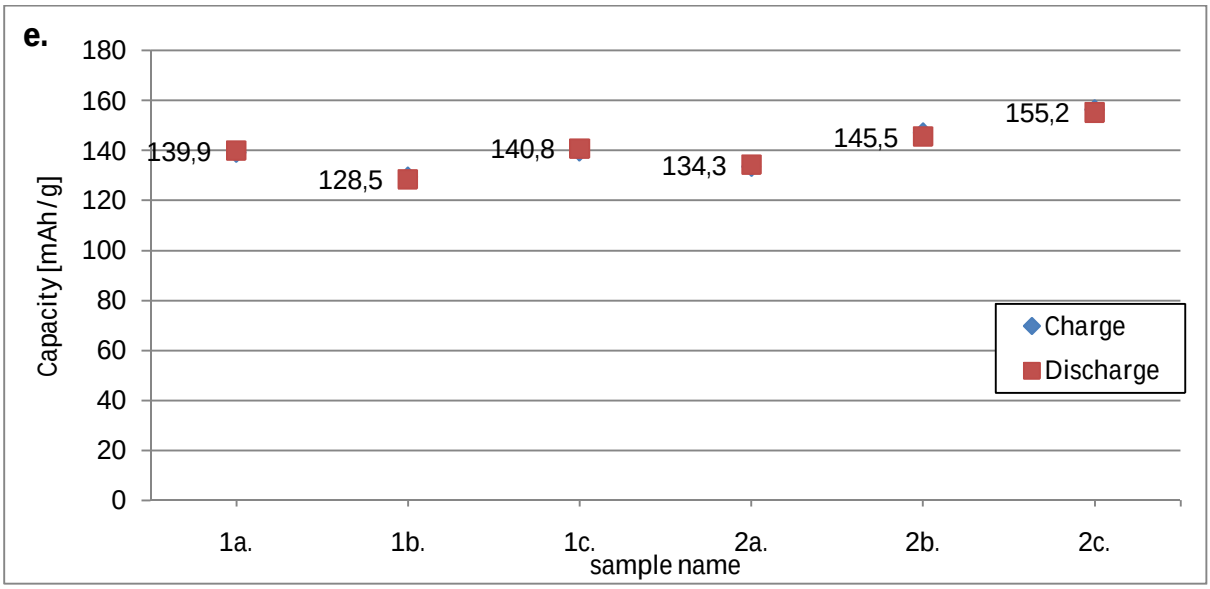

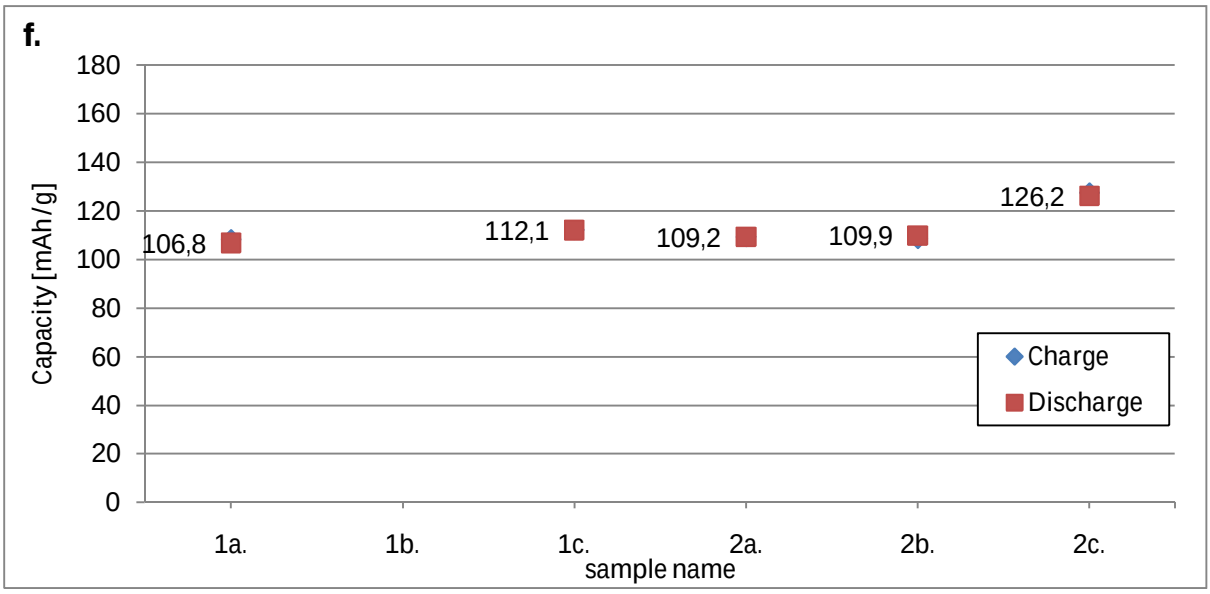

Fig.17. The fifth charge and discharge capacities of the prepared cells at; (e.) 0.1C rate and (f.) 1Crate. The presented data labels are related to the discharge capacities.

To investigate the electrochemical performance properties such as capacity retention, cycle life and cycle ability, a charge-discharge test was performed on sample 1b up to 390 cycles at 1C rate over the same voltage range. The long term results are presented with every 50 cycles in figure 18. The initial discharge capacity was measured to 109 mAh/g, while it increased to 118 mAh/g after 390 cycles. The results demonstrated

good capacity retention without any capacity fading on long term cycling. The increase in capacity after 50th cycle is most probably due to the temperature of the cell. As the cycling test proceed at a high current rate the temperature of the cell increases which reduces the electrolyte viscosity and enhances the lithium-ion diffusion and hence results in higher specific capacity.

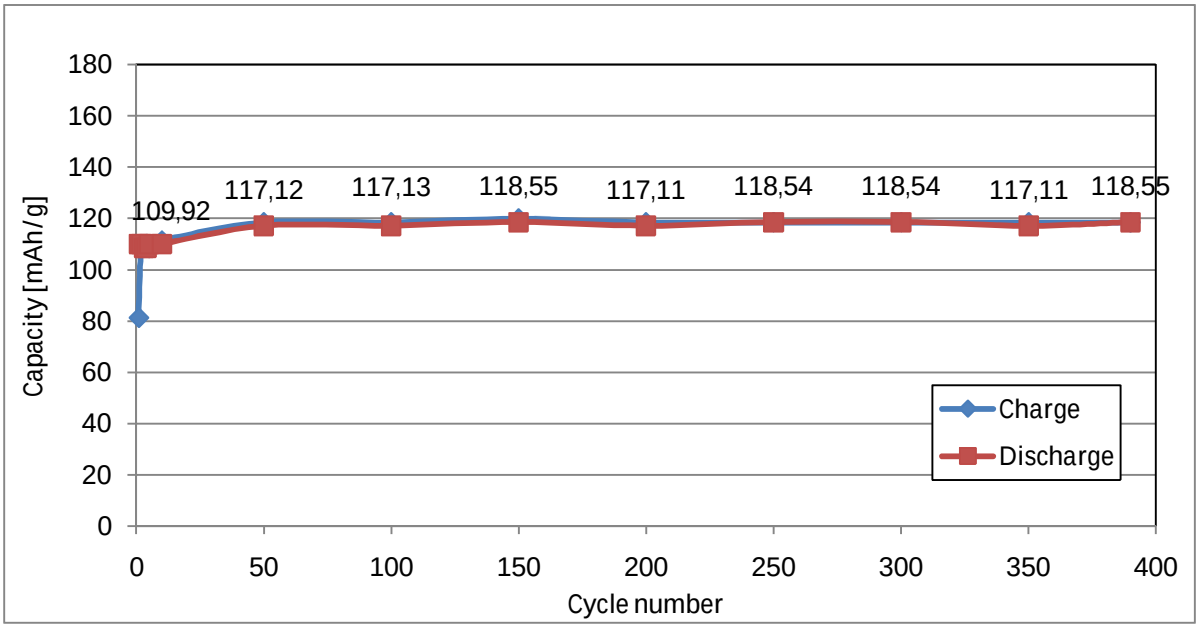

Fig.18. Long term cycle performance of sample 2b at 1C rate over the voltage of 2.7-4.2V. The results are presented for 1-5th, 10th and every 50th cycles. The data labels are presenting the discharge capacities.

For comparison, cycling tests were also performed on cathode materials based with commercial powder A at 0.1C rates between 2.7-4.2 V, as shown in figure 19. The cathode production method was the same as for the freeze granulated powder. The sample produced with the water based system contained 90 wt% $LiFePO_4$, 6 wt% carbon black and 4 wt% styrene butadiene rubber, whereas the sample made by NMP system contained 90 wt% $LiFePO_4$, 5 wt% carbon black and 5 wt% PVDF. The resulted discharge capacity was 155 mAh/g for water based cathode production and 160 mAh/g for NMP based cathode production at 0.1C rate.

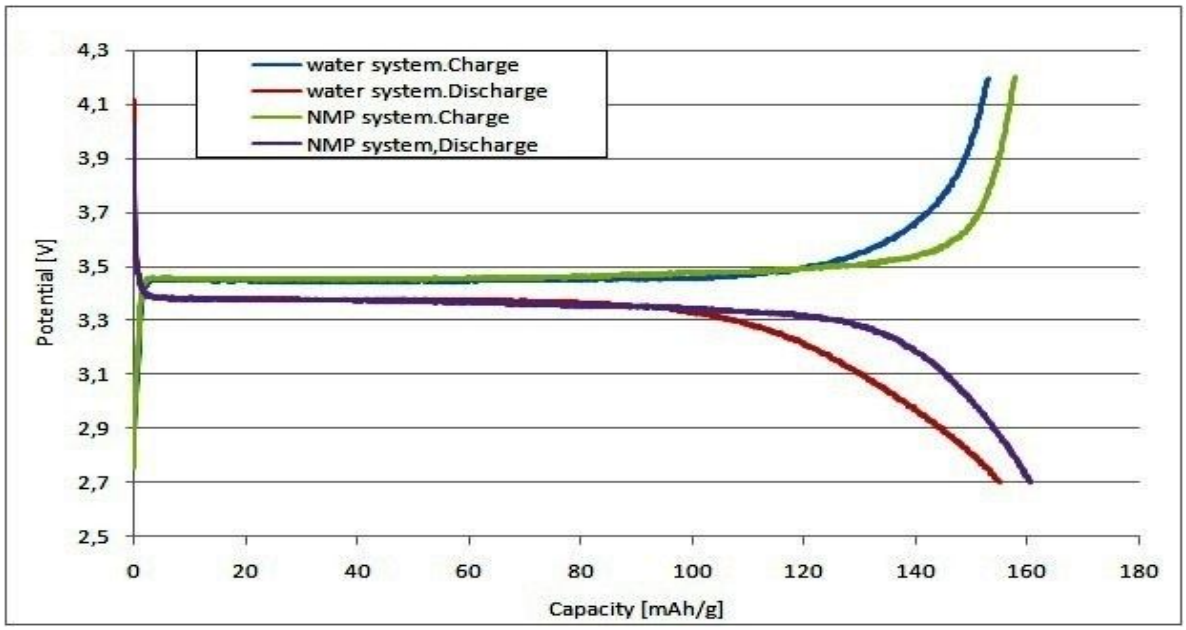

Fig. 19. Voltage profile of the fifth cycle of commercial powder A with water and NMP system cathode preparation at 0.1C rate.

The higher amount of active material and lower amount of binder used in the preparation of the commercial powder A are possible reasons to its higher capacity at 0.1C rate. More amounts of active material in cathode with an optimal amount of additives increases the specific capacity of the electrode and hence of the cell. The particle size (related to the specific surface area) of the commercial powder A was larger than the produced powder which made it possible to use less binder and provide a good adhesion to form the cathode electrode, therefore resulting in increased specific capacity.

5. Summary and Conclusions

In this study, the freeze granulation route was evaluated for the synthesis of $LiFePO_4$ cathode material using three types of precursor combinations. Poly vinyl alcohol (PVA) was used as a carbon source precursor prior to the calcination in order to enhance the conductivity and inhibit the grain growth of particles during calcination. The freeze granulation process was used in order to maximize the homogeneity of the precursor granules prior to calcination, done in temperature range of 600-800°C for 10 hour in nitrogen or argon + 10% hydrogen atmosphere. The influence of precursor combination, PVA content, calcination temperature and atmosphere were investigated regarding the structure, surface area, morphology and conductivity of the prepared $LiFePO_4/C$ powders. In order to compare the results two commercial $LiFePO_4/C$ powders were also evaluated in the same way as the produced materials. SEM results revealed that the carbon covered all the nano-size active material grains and formed an optimum continues network in the form of a thin film which increased the active material conductivity. The $LiFePO_4/C$ sample which was made from the second precursor combination (Li_2CO_3, $FeC_2O_4*2H_2O$ and $NH_4H_2PO_4$) and calcined for 10 hours at 700°C in Ar+10%H_2, revealed a high degree of purity, homogeneity and $LiFePO_4$ crystallinity according to the XRD result. This $LiFePO_4/C$ composite also showed a high specific surface area and SEM investigation revealed a nanostructure considered promising for cathode manufacturing and cell assembling. Cathodes were fabricated by manual tape casting with two different $LiFePO_4/C$ suspensions, based on water and N-methylpyrrolidone (NMP) respectively, on an aluminum foil. The produced cells in our experiment exhibited a relatively good specific capacity. The highest discharge capacity obtained for the NMP system cathode production was 155 mAh/g at 0.1C and 126 mAh/g at 1C rate as well as 140 and 112 mAh/g for the water system. The long-term stability test indicated good result with no loss in capacity for at least 390 cycles at 1C rate. The produced powders have shown good physical and electrochemical properties in comparison with tested commercial powders which were two of the best available powders on the market, currently. These promising results are due to the homogeneity of the $LiFePO_4/C$ active material supported by the freeze granulation process and enhanced electronic conductivity from an adapted carbon coating.

6. Future works

For the future there are still a number of actions of interest to further develop the performance of derived $LiFePO_4/C$ cathode material via the utilization of freeze granulation. It would be of interest to investigate alternative types of carbon source in order to optimize the ultimate carbon content, distribution and consistency.

Further, it might be possible to process the calcined powder without post-milling and granulation by alter and optimize the granule size in the initial granulation prior to calcination. Milling may affect the carbon distribution and limit its role as conductivity agent. Other factors such as calcination time, temperature and atmosphere have also to be further investigated.

For the water based cathode suspension preparation, it would be of interest to find alternative polymeric compositions for the application to improve the internal strength within the cathode material as well as the adhesion to the aluminum foil with less amount of binder, hence enhance the cell performance. Optimized granules size prior to calcination and exclusion of pre-milling prior to paste preparation for tape casting might contribute to this purpose.

7. References

[1] A.K. Padhi, K.S. Nanjundaswamy, J.B. Goodenough, J. Electrochem. Soc. 144 (1997) 1188.

[2] G. Cheruvally, (2008) Lithium iron phodphste: a promising cathode-active material for lithium secondary batteries. Switzerland : Trans tech publications Ltd.

[3] H.A. Keihne, (2003) Battery technology handbook. New York: Marcel Dekker.

[4]H. Gu, D. Jun, G. Park, B. Jin and E. Jin. (2007). Nanosized $LiFePO_4$ cathode materials for lithium ion batteries. J. Nanoscience and Nanotechnology. Vol 7. pp. 3980-3984.

[5] Source:http://bioage.typepad.com/.a/6a00d8341c4fbe53ef01156e4e74b5970c-popup [accessed 8/09/2011]

[6] S.Y .Chung, J.T .Bloking, and Y.M.Chiang, *Nat. Mater.* 1, 123 (2002).

[7] M.M. Doeff, Y. Hu, F. McLarnon, R. Kostecki, Electrochem. Solid-State Lett. 6 (2003) A207.

[8] R. Dominko, M. Bele, M. Gaberscek, M. Remskar, D. Hanzel, S. Pejovnik, J. Jamnik, J. Electrochem. Soc. 152 (2005) A607.

[9] H. Huang, S.-C. Yin, L.F. Nazar, Electrochem. Solid-State Lett. 4 (2001) A170.

[10] A. Yamada, S.C. Chung, K. Hinikuma, J. Electrochem. Soc. 148 (2001) A224.

[11] L.N. Wang a, X.C. Zhana, Z.G. Zhang a and K.L. Zhang. (2008). A soft chemistry synthesis routine for LiFePO4–C using a novel carbon source. J. Alloys and Compounds. Vol 456. pp. 461-465.

[12] N. J. Yun, H. W. Ha, K. Jeong, H.Y. Park and K. Kim. (2006). Synthesis and electrochemical properties of olivine-type LiFePO4/C composite cathode material prepared from a poly vinyl alcohol-containing precursor. J. Power Sources. Vol 160. pp. 1361–1368.

[13] S. Luo a,b, Z. Tang a, J. Lu a and Z. Zhang. (2008). Electrochemical properties of carbon-mixed LiFePO4 cathode material synthesized by the ceramic granulation method. J. Ceramics International. Vol 34. pp. 1349–1351.

[14] D.Wang, H. Li, Z.Wang, X.Wu, Y. Sun, X. Huang, L. Chen, J. Solid State Chem. 177 (2004) 4582.

[15] C.H. Mi, X.B. Zhao, G.S.Cao and J.P.Tu: J.Electrochem. Soc. Vol. 152 (2005), P.A 483.

[16] W. Porcher, B. Lestriez, S. Jouanneau and D. Guyomard. (2009). Design of Aqueous Processed Thick LiFePO4 Composite Electrodes for High-Energy Lithium Battery. J. Electrochemical Society. Vol 156. pp. 133-144.

[17] M. Zackrisson, L. Avellán, J. Orlenius. (2010). Life cycle assessment of lithium-ion batteries for plug-in hybrid electric vehicles - Critical issues. J. Cleaner Production. Vol 18. pp. 1517-1527.

[18] J. Li, C. Daniel and D. Wood. (2011). Materials processing for lithium-ion batteries. J. Power sources. Vol 196. pp. 2452-2460.

[19] K. Rundgren, O. lyckfelt, M. Sjöstedt: Improving powders with freeze granulation, Ceramic Industry, April, 40-44, 2003.

[20]Source:http://powderpro.se/wp/wp-content/uploads/2011/05/freeze-granulation-illustration.jpg [accessed 8/09/2011]

[21] Source: http://powderpro.se/wp/wp-content/uploads/2011/05/freeze-granulation-vs-spray-drying.jpg [accessed 8/09/2011]

[22] N. Trsic-Milanovic, A. Kodzic, J.Baras and C. Dimitrijevic-Brankovic. The influence of a cryoprotective medium containing glycerol on lyphilization of latic acid bacteria. J. serb.chem.soc. No 2872, pp. 435-441.

[23] J.W. Gilman, D.L. VanderHart and T. Kashiwagi. (1994). Fire and polymers II: materials and test for hazard prevention, in: ACS Symposium Series 599, American Chemical Society, Washington, DC, p.161 (Chapter 11).

[24] F. Gao, Z. Tang and J. Xue. (2007). Preparation and characterization of nano-particle LiFePO4 and LiFePO4/C by spray-drying and post-annealing method. J. Electrochemica acta. Vol 53. pp. 1939–1944.

[25] A. Xinping, L. HaP, L. Xiaoyaff, L. Qinlin, L. Bingdong and Y. Hanxi. (2006). One Step Ball-Milling Synthesis of LiFeP04 Nanoparticles as the Cathode Material of Li.lon Batteries. J. WUJNS. Vo1 11, No 3, pp. 687-690.

[26] S. Franger, F. Le Cras, C. Bourbon and H. Rouault. (2003). Comparison between different LiFePO4 synthesis routes and their influence on its physico-chemical properties. J. Power Sources. Vol 119-121. pp. 252–257.

[27] Y. Xia, M. Yoshio and H. Noguchi. (2006). Improved electrochemical performance of LiFePO4 by increasing its specific surface area. J. Electrochimica Acta. Vol 52. pp. 240–245.

[28] High-Tech Productions / Blank Video Tape.com. (2010)Glossary of Battery Terms. http://www.high-techproductions.com/glossary1.htm [accessed 8/09/2011].

[29]Source: http://powderpro.se/wp/wp-content/uploads/2011/05/lab-scale-granulator.jpg [accessed 8/09/2011]

Appendix A. XRD results

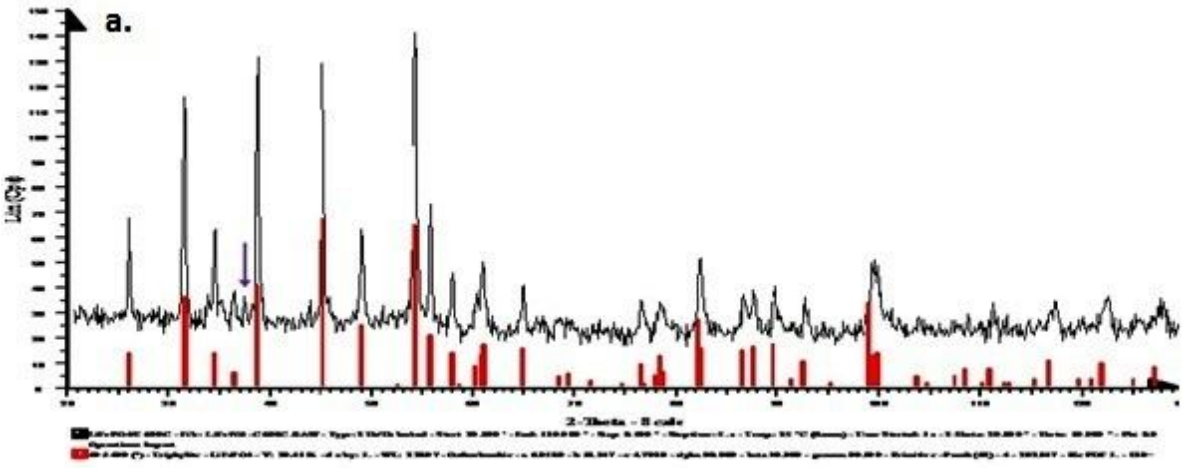

a) $LiFePO_4/C$, first precursor combination,600°C&10h, 5% PVA , N_2

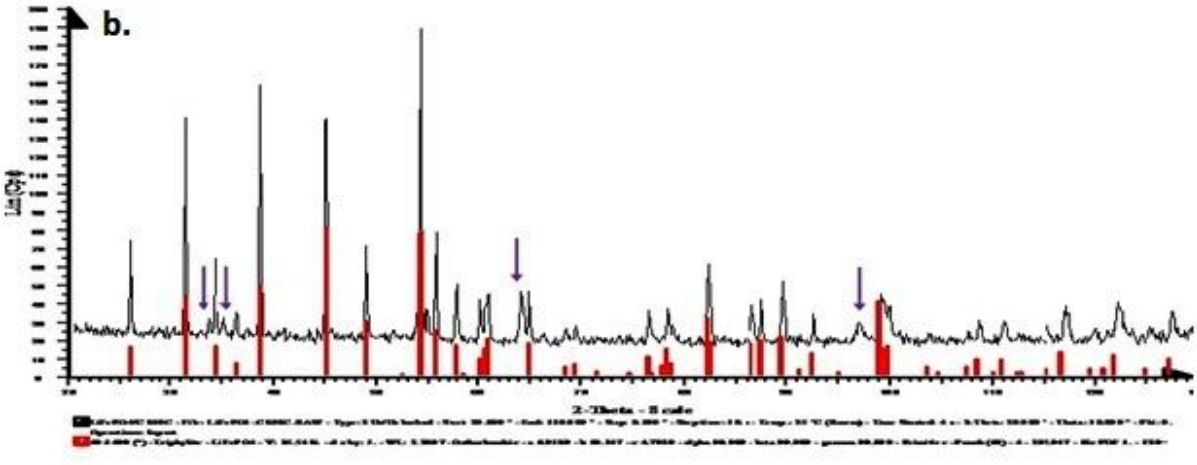

b) $LiFePO_4/C$, first precursor combination,800°C&10h, 5% PVA , N_2

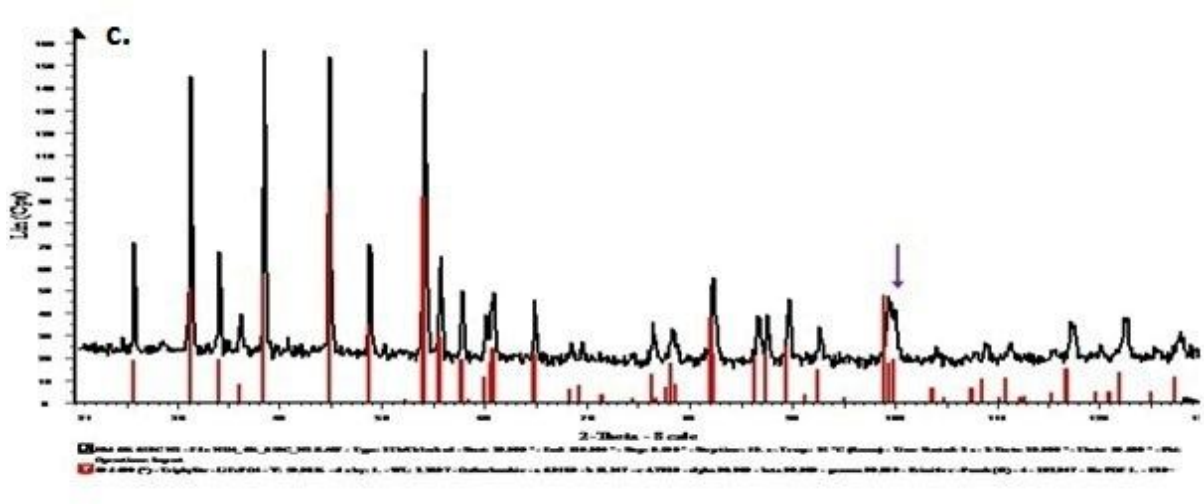

c) $LiFePO_4/C$, second precursor combination,650°C&10h, 6% PVA , N_2

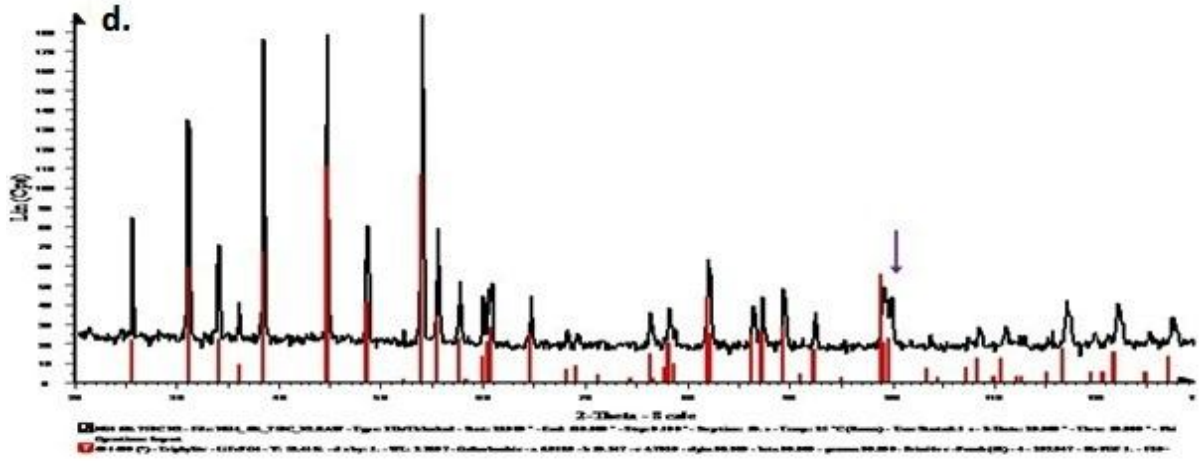

d) $LiFePO_4/C$, second precursor combination,750°C&10h, 6% PVA , N_2

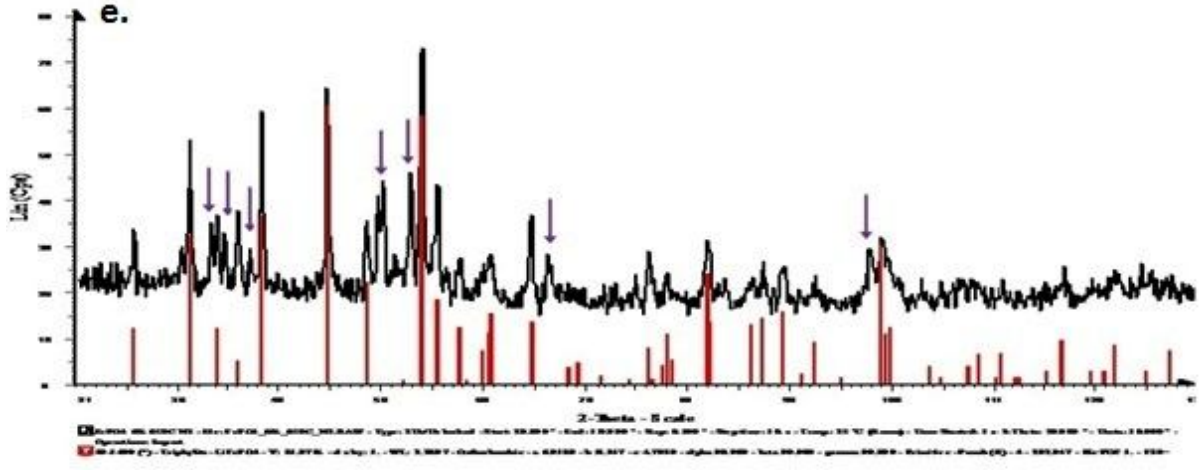

e) $LiFePO_4/C$, third precursor combination,650°C&10h, 6% PVA , N_2

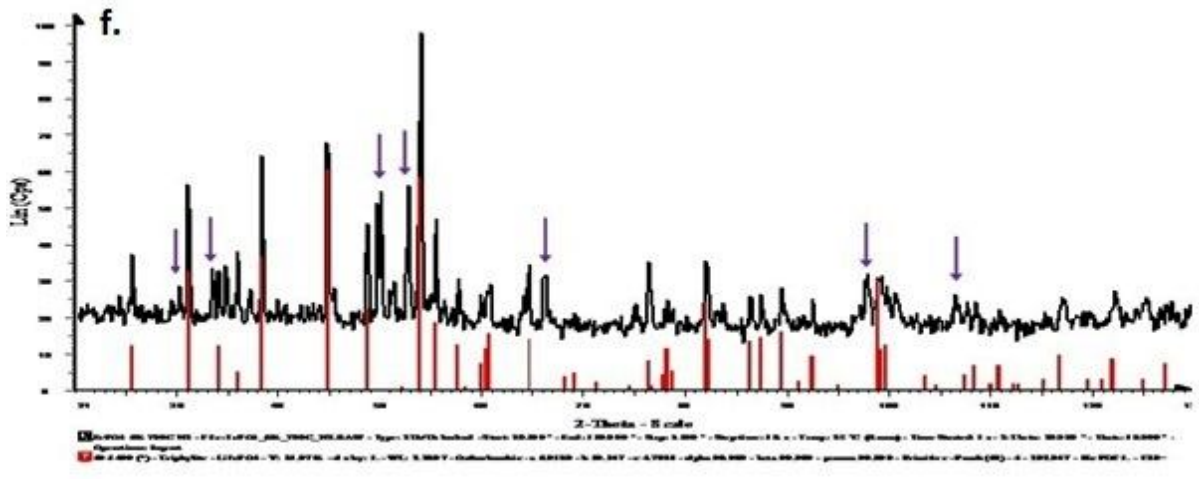

f) $LiFePO_4/C$, third precursor combination,700°C&10h, 6% PVA , N_2

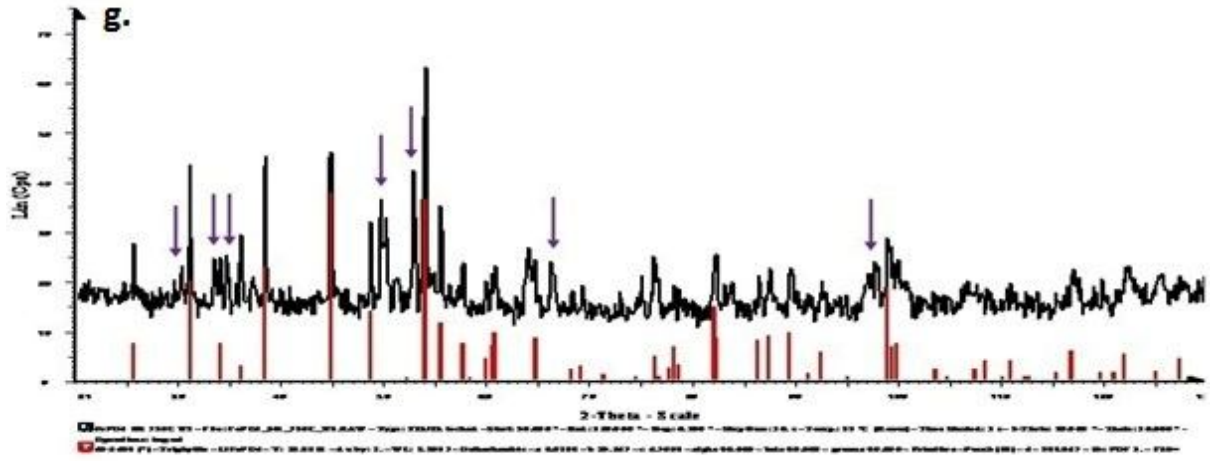

g) $LiFePO_4/C$, third precursor combination,750°C&10h, 6% PVA , N_2